



Universität Bremen



ALFRED-WEGENER-INSTITUT
HELMHOLTZ-ZENTRUM FÜR POLAR-
UND MEERESFORSCHUNG

The physiological response of an Arctic key species
Polar cod, *Boreogadus saida*, to environmental
hypoxia: critical oxygen level and swimming
performance



Sarah Kempf

Master Thesis

University of Bremen

First Supervisor: Dr. Felix Christopher Mark (AWI)

Second Supervisor: Dr. Andreas Kunzmann (ZMT)

Edited Version: February 18th 2020

Table of contents

List of Figures and Tables	i
Figures	i
Tables	v
List of Abbreviations	vi
Summary	viii
Zusammenfassung	x
1 Introduction	1
1.1 Study animal	2
1.2 Study area under climate change	3
1.3 Physiological background	8
2 Material and methods	10
2.1 Fish tagging	10
2.2 SMR and RMR measurements	11
2.3 Swimming performance measurements	13
2.4 Data handling	15
2.4.1 Oxygen consumption	15
2.4.2 Normalized oxygen consumption	16
2.4.3 Standard metabolic rate	16
2.4.4 Routine metabolic rates	16
2.4.5 Maximum metabolic rates	17
2.4.6 Aerobic scope	17
2.4.7 Critical swimming speed (U_{crit}) after Brett (1964)	17
2.4.8 Gait transition speed (U_{gait})	18
2.4.9 Troubleshooting	18
2.4.10 Statistical analysis	18
3 Results	19
3.1 Mortality	19
3.2 Respiration measurements	19
3.2.1 Standard metabolic rate	19
3.2.2 Standard and routine metabolic rate	20
3.2.3 Standard and maximum metabolic rate	22
3.2.4 Standard-, routine-, maximum metabolic rate and aerobic scope	23
3.2.5 LOL curve and P_{crit}	25
3.3 Swimming performance	26
3.3.1 MR at different water velocities	26
3.3.2 Gait transition speed U_{gait}	27

3.3.3	Critical swimming speed (U_{crit})	29
4	Discussion	31
4.1	Respiration measurements.....	31
4.2	Swimming performance	37
5	Conclusion.....	40
6	References	xii
	Appendix	xxii
	Acknowledgements – Danksagung	xxxv

List of Figures and Tables

Figures

- Figure 1 Study area Billefjorden (Svalbard archipelago).** **A:** position of the Svalbard archipelago on a world map. **B:** position of the Svalbard archipelago in context of mainland. **C:** enlarged map of the Svalbard archipelago. **D:** exact position of Billefjorden. 3
- Figure 2 Comparison Kongsfjorden and Billefjorden.** Upper row: depth profile of Kongsfjorden (04.10.2018) (11.6928°E, 78.9840°N), Lower row: depth profile of Billefjorden (06.10.2018) (16.4997°E, 78.5883°N), plots from left to right: temperature (°C), salinity (psu) and oxygen saturation (%) with increasing depth. (Data from: Mark and Wisotzki 2018). 4
- Figure 3 Projected changes from 1961–90 to 2071–2100 in mean annual temperature (°C)** The RCM projections are based on MPIB2 (for acronyms, see Appendix Table 12; for weather stations used in the analysis, see Appendix Figure 21) (Førland, Benestad et al. 2011). 5
- Figure 4 Temperature projections for Svalbard Airport/Longyearbyen:** results from ESD and RCM downscalings for winter, spring, summer, and autumn. The hatched area (pink) shows 5 % and 95 % interval from ESD estimates, the black dots show observed values, and the thick line (red) show median (50 %) value for the ESD ensemble. The coloured symbols indicate the median value for the different runs with NorACIA-RCM, and the vertical lines show the 5- and 95-percentiles for the RCM runs. The RCM values are plotted on the central year in the respective time slices. (for acronyms, see Appendix Table 12; for weather stations used in the analysis, see Appendix Figure 21) (Førland, Benestad et al. 2011). 6
- Figure 5 Hydrographic profile along the main axis of Billefjorden (August 2001)** **A:** salinity, **B:** Water masses are marked by a dotted line, the shaded area marks land masses; SW – surface water, IW – intermediate water, LW – local water, WCW – winter-cooled water (modified after Szczuciński, Zajączkowski et al. 2009). 7
- Figure 6 Limiting oxygen level (LOL) curve.** The ambient oxygen saturation [%] influences the aerobic metabolic capacity of an idealized organism (modified after Claireaux and Chabot 2016). Shown are the maximum sustainable metabolic rate (MMR) (red dashed line) and standard metabolic rate (SMR) (green dashed line), the LOL curve (black), aerobic scope (distance between LOL curve and SMR) and the critical oxygen level (P_{crit}) (Neill and Bryan 1991, Claireaux and Chabot 2016). 9
- Figure 7 Schematic construction of the respirometry system.** All respiration chambers are connected to one recirculation pump and one flush pump. Within the recirculating water, flow probe vessels are included where the oxygen probes are located. A four-channel oxygen meter (Loligo systems ApS, Denmark, Witrox 4 oxygen meter for mini sensors) detects the ambient oxygen in the chambers and basin as well as temperature, sending the data via Bluetooth to a

computer with the software AutoResp version 2.3.0 (Loligo Systems ApS, Denmark). Compressed air (CA) together with nitrogen (N₂) create the desired oxygen concentration (100 - 5 % saturation). The data acquisition instrument (DAQ-M) controls the flush and recirculation pumps and the amount of nitrogen pumped into the water. DAQ-M is also connected to and controlled by a computer with the software AutoResp. 12

Figure 8 Schematic construction of the swim tunnel A four-channel oxygen meter (Loligo systems ApS, Denmark, Witrox 4 oxygen meter for mini sensors) detects the ambient oxygen in the swim tunnel as well as temperature, sending the data via Bluetooth to a computer with the software AutoResp version 2.2.0 (Loligo Systems ApS, Denmark). Compressed air (CA) together with nitrogen (N₂) create the desired oxygen concentration (100 – 10 % oxygen saturation). The data acquisition instrument (DAQ-M) controls the flush pump and the amount of nitrogen pumped into the water. DAQ-M is also connected to and controlled by a computer with the software AutoResp. A motor regulated by the controller drives the propeller, creating a laminar current within the swim tunnel. The fish is placed in the operation part of the tunnel. 14

Figure 9 Standard metabolic rate (SMR). Shown are the metabolic rates ((MR) in $\mu\text{mol O}_2/\text{g}\cdot\text{h}$) (orange circles) recorded at 56 - 100 % PO₂. The SMR (0.44 $\mu\text{mol O}_2/\text{g}\cdot\text{h}$; black line) was calculated as described under point 2.4.3 using the R package “Mclust” after Chabot et al. (2016). 19

Figure 10 Routine metabolic rate (RMR). Shown are the metabolic rates ((MR) in $\mu\text{mol O}_2/\text{g}\cdot\text{h}$) (orange circles) (86 experimental runs representing 1887 single metabolic rate data points of 30 individuals) performed between 5 and 100 % PO₂ in respiration chambers. The RMR (dark orange line, with SD (light orange area)) was calculated as described under point 2.4.4. Black line: standard metabolic rate (SMR; 0.44 $\mu\text{mol O}_2/\text{g}\cdot\text{h}$). 20

Figure 11 Maximum metabolic rate (MMR). Shown are the metabolic rates ((MR) in $\mu\text{mol O}_2/\text{g}\cdot\text{h}$) (blue circles) (60 experimental runs representing 361 single metabolic rate data points of 30 individuals) performed between 10 and 100 % PO₂ in the swim tunnel. The MMR (dark blue line, with SD (light blue area)) was calculated as described under point 2.4.5. Black line: standard metabolic rate (SMR; 0.44 $\mu\text{mol O}_2/\text{g}\cdot\text{h}$). 22

Figure 12 Routine- (RMR), maximum- (MMR) and standard metabolic rate (SMR) of 148 single measurements with a total of 30 multiple used individuals. Metabolic rates ((MR) in $\mu\text{mol O}_2/\text{g}\cdot\text{h}$) at the different oxygen saturation (%). Data from both, swim tunnel and respiration chamber, experiments. In blue: metabolic rate of 60 individuals recorded during swim tunnel experiments. In orange: metabolic rate of 86 individuals recorded during measurements in respirometry chambers. Upper blue line: maximum metabolic rate (swimming tunnel; calculated as described in 2.4.5). Lower dark orange line: routine metabolic rate (respiration chambers; calculated as described in 2.4.4). Black line: SMR (respiration chambers; calculated as described in 2.4.3). Grey shaded area: aerobic scope (difference between MMR and RMR)..... 24

- Figure 13 Aerobic scope.** Bars represent the mean aerobic scope of Polar cod at ten different oxygen saturations (treatments). The different grey shadings represent three significantly different levels of AS. Aerobic scope was calculated as described in 2.4.6. Error bars depict standard deviation. *Asterisks:* significant difference between the three decreasing levels of AS (***, or a, b, c for the three steps), all p-values are lower than 0.0001. 24
- Figure 14 Limiting oxygen level (LOL) curve after Claireaux and Chabot (2016).** Shown are the maximum metabolic rate (MMR; blue line) and standard metabolic rate (SMR; black line), MMR regression line (dashed blue line; polynomial regression of the MMR between 10.77 and 25.36 % PO₂ ($y = 1E-06x^2 + 0.0002x - 0.0005$; $R^2 = 0.9994$)), the critical oxygen level (P_{crit} (4.81 %), red circle, intersection between MMR regression line and SMR) and the scope of survival (between 1.71 and 4.81 % PO₂)..... 25
- Figure 15 Metabolic rates over increasing water velocities.** Boxplots (with median and outliers) show the results of the swim tunnel measurements. Displayed are the MR [mmol O₂/g·h] during increasing water velocities [BL/sec]. Letters indicate results of Tukey honest significance test between Velocity treatments. Significant differences are represented by different letters, the corresponding p-values can be found in Table 3.(n per velocity: 1.40=59, 1.55=59, 1.70=60, 1.85=56, 2.00=45, 2.15=38, 2.30=21, 2.45=12, 2.60=8, 2.75=2, 2.90=1)..... 26
- Figure 16 Gait transition speed (U_{gait}) over increasing oxygen concentrations.** Comparison of U_{gait} (BL/sec) at different oxygen levels (n per treatment: 10=1, 15=2, 20=3, 25=6, 30=6, 40=5, 50=6, 60=6, 70=6, 100=6). No significance between PO₂ treatments was observed. 28
- Figure 17 Critical swimming speed (U_{crit}) over increasing oxygen concentrations.** Comparison of U_{crit} (BL/sec) at different oxygen levels (n:6 per treatment). Letters indicate results of Tukey honest significance test between PO₂ treatments (p= 0.031). All other p-values can be found in Table 6. 29
- Figure 18 Turbine calibration.** The turbine rotation was calibrated using a flowmeter. Turbine rotation was increased in steps of 10 rpm, de corresponding water velocity in m/s were detected with a flowmeter. Water velocity was measured at the bottom of the working section in the swim tunnel. This was repeated randomly for the middle and top layer of the working section. Linear regressions though the values measured in the middle and top region to calculate the corresponding water velocity at 1020 rpm. This calibration data was used to determine the actual water velocity within the swim tunnel. xxiii
- Figure 19 P_{crit} calculation.** Shown are SMR (black), RMR (orange), MMR (blue), RMR linear regression line (dotted orange) and MMR polynomial regression line (dotted blue)..... xxiii
- Figure 20 P_{crit} of marine species grouped by temperature range -1.5 to 20°C.** Values represent the respective mean P_{crit} (\pm SE). Numbers contained within each bar indicate the temperature (°C) at which P_{crit} was determined. Blue shaded bars mark data of Polar- or Gadidae species, relevant

for this study. Yellow bar: P_{crit} of *B. saida* determined in this study and included in this database (modified after Rogers et al. 2016)..... xxxii

Figure 21 **Map of the Svalbard region including weather stations used in the analysis** (Førland, Benestad et al. 2011). xxxiii

Figure 22 **Annual temperature development at weather stations in the Svalbard region.** The lowpass filtered series are smoothed by Gaussian weighting coefficients and show variability on a decadal time scale. The curves are cut three years from start and end (Førland, Benestad et al. 2011). xxxiv

Figure 23 **Collection of metabolic scopes** of European sea bass (*Dicentrarchus labrax*), Atlantic cod (*Gadus morhua*), common sole (*Solea solea*) and turbot (*Psetta maxima*) as a function of ambient dissolved oxygen. MS is shown on absolute scale (a) and relative to normoxia (b) (Chabot and Claireaux 2008). xxxiv

Tables

Table 1	P-values of TukeyHSD, RMR. Comparison of all treatments and the corresponding metabolic rates from respirometry chambers. Significant p-values are printed in bold type. Treatments 10 and 5% PO ₂ have been repeated due to recalibration of the oxygen optodes.....	21
Table 2	P-values of TukeyHSD, MMR and PO₂. Comparison of all treatments and the corresponding metabolic rates from swim tunnel. Significant p-values are printed in bold type.	23
Table 3	P-values of TukeyHSD, MMR and velocity. Comparison of all velocity treatments and the corresponding metabolic rates from swim tunnel. Significant p-values are printed in bold type.	27
Table 4	Burst activity. Mean total number of bursts (with standard deviation, SD) and mean bursts per minute (with SD) of all fish ordered by PO ₂ treatments.....	28
Table 5	Swimming activity. Mean percentage of active (with standard deviation, SD) and inactive phases (with SD) and the mean of the total swim time [min] (with SD) during the swim tunnel experiments ordered by PO ₂ treatments.	30
Table 6	P-values of TukeyHSD, U_{crit} and PO₂. Comparison of all treatments and the corresponding metabolic rates from swim tunnel. Significant p-values are printed in bold type.	30
Table 7	Fish-tagging. Serial number of the implanted passive glass transponder (PIT), the fish weight [g], total- and standard length [cm], width [cm] (vertical axis, measured at the thickest point) and depth [cm] (horizontal axis, measured at the thickest point).....	xxii
Table 8	U_{gait} [rpm and BL/sec] and U_{crit} [rpm and BL/sec] for all fish ordered by the different PO ₂ treatments.....	xxiv
Table 9	Raw data bursts. Ordered by PO ₂ Treatments, TSB = time spent bursting.....	xxvi
Table 10	Raw data swimming time. Ordered by PO ₂ Treatments, TMT = total measurement time, sec. inactive = inactive period per fish in seconds during measurement time.....	xxix
Table 11	Average annual and seasonal temperatures (°C) during 1961–90 and 1981–2010 (Førland, Benestad et al. 2011).....	xxxiii
Table 12	RCM simulations for the Svalbard region. The simulations were performed by the regional climate model HIRHAM2/NorACIA (Førland, Flatøy et al. 2009, Førland, Benestad et al. 2011).	xxxiv

List of Abbreviations

α	O ₂ solubility coefficient after Boutilier et al. 1984
μmol	micromole
ANOVA	analysis of variance
AS	aerobic scope
AWI	Alfred-Wegener-Institute Helmholtz Center for Polar and Marine Research
<i>B. saida</i>	<i>Boreogadus saida</i> , Polar cod
BL	body length
BW	body weight
CO ₂	carbon dioxide
EPOC	post-exercise oxygen consumption
HPLC	high performance liquid chromatography
IPCC	Intergovernmental Panel on Climate Change
IW	intermediate water
LOL	limiting oxygen level
LW	local water
mmol	millimole
MMR	maximum metabolic rate
MO ₂	oxygen consumption
O ₂	molecular oxygen
OCLTT	oxygen & capacity limited thermal tolerance
PCO ₂	carbon dioxide partial pressure
PO ₂	oxygen partial pressure
ΔPO_2	change in water PO ₂ [kPa]
p_{MMR}	p-values for the swim tunnel experiment
P_{RMR}	p-values for the respirometry chamber experiment
RMR	routine metabolic rate
rpm	rotations per minute
SMR	standard metabolic rate
SW	surface water
t	time interval
Δt	elapsed time
T	time spent at the given velocity leading to exhaustion of the fish

Temp.	temperature
U_{crit}	critical swimming speed (maximum achievable swimming speed)
U_{gait}	gait transition speed (transition phase of purely aerobic and partly anaerobic swimming)
U_{max}	highest velocity (v) perpetuated for a complete time interval (t)
v	velocity
V	volume
WCW	winter cooled water

Summary

Since the beginning of the industrialization, uncontrolled greenhouse gas emission led to a distinct temperature increase on earth. Arctic environments are projected to experience the most severe changes due to climate change. Higher atmospheric temperatures caused already various environmental changes, for example a decrease in Arctic sea ice of 49 % (1979-2000) and increasing carbon dioxide concentrations which reduced the sea surface pH. A reduced sea ice formation will strengthen the summer stratification of warm, oxygen poor on top of cold, oxygen rich water masses, which may consequently cause local hypoxia in ground water layers. As a result, the deep cold water layers do not receive oxygen-rich water and oxygen consumption extends over more than one season. This can lead to local hypoxia in the ground water layers of the protected fjords. Especially endangered of this long-lasting stratification in winter are the deep fjord systems of the Svalbard archipelago. In this region, the change of winter temperatures from 1961–90 corresponded to an increase of 0.6 °C per decade. Corresponding, an additional increase of 0.9 °C per decade is projected for 2071–2100. Thus, the present study investigates the hypoxia tolerance of Polar cod, *Boreogadus saida*, one of the main Arctic key species. Therefore, different performance parameters were determined. The respiratory capacity as well as the swimming performance under declining oxygen concentrations were measured in two different experimental setups. A sample size of 30 Polar cod with similar body length and weight were chosen. All individuals were used several times during the experiments. First, the routine (RMR) and standard metabolic rate (SMR) were determined via flow-through respirometry. The calculated SMR for Polar cod accounted 0.44 $\mu\text{mol O}_2/\text{g}\cdot\text{h}$. The RMR followed an oxygen regulating pattern, indicating that aerobic metabolic pathways such as lipid oxidation were used, rather than anaerobic pathways. This implies a relatively small contribution of anaerobic metabolism to the energy production in *B. saida*. This was confirmed in the swim tunnel experiments. However, U_{gait} (the speed at which the fish changed to anaerobically fuelled swimming) was not significantly affected by hypoxia, the total number of bursts ($p = 0.025$) and total active swimming time ($p = 0.017$) significantly decreased with decreasing oxygen saturation. The loss of anaerobic swimming capacity due to hypoxia may endanger this species in regard to predator-prey-interactions and loss of escape reactions. Under exercise Polar cod was able to up-regulate its maximum metabolic rate (MMR) until a threshold of 45 % PO_2 was reached. Afterwards, the oxygen consumption significantly decreased with decreasing oxygen concentrations. Throughout both experiments neither RMR nor MMR decreased below SMR level. Furthermore, the present study revealed that Polar cod

is an extremely hypoxia tolerant fish species, which is able to handle oxygen saturations down to a P_{crit} of 4.81 % PO_2 . This outstanding capability could give the otherwise rather disadvantaged fish species an advantage under changing climate conditions.

Zusammenfassung

Seit Beginn der Industrialisierung führte der unkontrollierte Ausstoß von Treibhausgasen zu einem deutlichen Temperaturanstieg auf der Erde. Für die Arktis werden die stärksten Veränderungen durch den Klimawandel prognostiziert. Höhere atmosphärische Temperaturen verursachten bereits verschiedenste Umweltveränderungen, wie zum Beispiel eine Abnahme des arktischen Meereises um 49 % (1979-2000) und steigende Kohlendioxidkonzentrationen, die den pH-Wert der Meeresoberfläche stark senkten. Eine verringerte Meereisbildung wird die sommerliche Schichtung von warmen, sauerstoffarmen und kalten, sauerstoffreichen Wassermassen verstärken, was zu einer lokalen Hypoxie in den Grundwasserschichten führen kann. Besonders gefährdet von dieser langanhaltenden Trennung der Wassermassen im Winter sind die tiefen Fjordsysteme des Svalbard-Archipels. In dieser Region entsprachen Temperaturveränderungen zwischen den Jahren 1961 und 1990 einem Anstieg um 0,6 °C pro Jahrzehnt. Anhand dieser Veränderung wird für den Zeitraum von 2071 bis 2100 ein weiterer Anstieg um 0,9 °C pro Jahrzehnt prognostiziert. Die vorliegende Studie untersucht daher die Hypoxie-Toleranz von Polardorsch, *Boreogadus saida*, einer der wichtigsten arktischen Schlüsselarten. Dazu wurden verschiedene Leistungsparameter ermittelt. Sowohl die Atmungskapazität als auch die Schwimmleistung bei abnehmenden Sauerstoffkonzentrationen wurden in zwei verschiedenen Versuchsaufbauten gemessen. Es wurde eine Probengröße von 30 Polardorschen mit ähnlicher Körperlänge und ähnlichem Gewicht gewählt. Alle Individuen wurden während der Experimente mehrfach verwendet. Zunächst wurden die Routine- und die Standard-Stoffwechselraten mittels Durchflussrespirometrie bestimmt. Der berechnete Standard-Stoffwechsel für den Polardorsch betrug 0,44 $\mu\text{mol O}_2/\text{g}\cdot\text{h}$. Der Routine-Stoffwechsel folgte einem sauerstoffregulierenden Muster, was darauf hinweist, dass aerobe Stoffwechselwege wie die Lipidoxidation genutzt wurden und anaerobe Stoffwechselwege für diese Arte eine kleinere Rolle spielen. Dies impliziert einen relativ geringen Beitrag des anaeroben Stoffwechsels zur Energieproduktion in *B. saida*. Dies wurde in den Schwimmtunnel-Experimenten bestätigt. Auch wenn U_{gait} (die Geschwindigkeit bei, der die Fische zu anaerob angetriebenem Schwimmen übergangen) nicht signifikant durch Hypoxie beeinflusst wurde, konnte ein signifikanter Zusammenhang zwischen einer sinkenden Gesamtzahl der Bursts ($p = 0,025$) sowie einer Abnahme der gesamten, aktiven Schwimmzeit ($p = 0,017$) mit abnehmender Sauerstoffsättigung gezeigt werden. Dieser Verlust der anaeroben Schwimmkapazität durch die Hypoxie kann diese Spezies in Bezug auf Raubtier-Beute-Interaktionen und den Verlust von Fluchtreaktionen unter zukünftigen Umweltbedingungen

stark gefährden. Unter Belastung konnte der Polardorsch seine maximale Stoffwechselrate hochregulieren, bis ein Schwellenwert von 45 % PO₂ erreicht wurde, danach nahm der Sauerstoffverbrauch mit abnehmender Sauerstoffkonzentration im Wasser signifikant ab. Während beider Experimente sanken die Stoffwechselraten nie unter das Niveau des Standard-Stoffwechsels. Darüber hinaus zeigte die vorliegende Studie, dass Polardorsch eine extrem hypoxietolerante Fischart ist, die mit Sauerstoffsättigungen bis zu einem P_{crit} von 4,81 % PO₂ umgehen kann. Diese hervorragende Fähigkeit könnte dieser sonst eher benachteiligten Fischart unter veränderten Klimabedingungen einen Vorteil verschaffen.

1 Introduction

Since the polar oceans are expected to warm twice as fast as the global average, polar key species such as *Boreogadus saida* are ideal model organisms to understand physiological responses to global warming and predicted future ecosystem scenarios (Hoegh-Guldberg and Bruno 2010, Hop and Gjørseter 2013, Fossheim, Primicerio et al. 2015). Changes in abundance of *B. saida*, either caused directly by ecological changes driven by global warming or indirectly by invasion of predators and competition among immigrating species, have grievous consequences on the whole ecological system (Craig, Griffiths et al. 1982, Welch, Bergmann et al. 1992, Orlova, Dolgov et al. 2009). Therefore, it is of great interest to determine the ecophysiological thresholds of this key species for the changing parameters in future climate scenarios. Based on the unknown physiological response of Polar cod to progressive hypoxia, three major questions arose. (1) Does progressive hypoxia influence its metabolic rate? (2) Does the swimming performance of Polar cod respond to diminishing oxygen availability? (3) In which oxygen range do we find the critical oxygen concentration (P_{crit}) concentration of Polar cod? To answer those questions, oxygen uptake and swimming performance were recorded as physiological performance parameters under progressive hypoxia. Concerning the swimming performance, I hypothesise that the critical swimming speed (U_{crit}) should be reached earlier with progressing hypoxia. Earlier studies showed that scant oxygen availability lowers the maximum metabolic rate (MMR) and therefore decreases the energy supply (Pörtner 2010). Compared with previous studies where polar cod was exposed to hypercapnia together with increased temperature, high sensitivities of maximum performance parameters (MMR, U_{gait} , U_{crit}) were revealed (Kunz, Claireaux et al. 2018). Comparing to other Gadidae species, Atlantic cod (*Gadus morhua*) reduced swimming speed by 21 – 41 % under hypoxia (20 – 40 % oxygen saturation) (Herbert and Steffensen 2005). Furthermore, based on studies on other Gadidae species as Atlantic cod (*Gadus morhua*) and Greenland cod (*Gadus ogac*) the P_{crit} of Polar cod can be assumed to be found between 25 and 40 % oxygen saturation (Steffensen, Bushnell et al. 1994, Rogers, Urbina et al. 2016) (Appendix Figure 20).

1.1 Study animal

The Polar cod (*Boreogadus saida* (Lepechin, 1774)) belongs to the family of Gadidae and is a generally small fish with an average maximum length of 30 cm (Scott and Scott 1988, Hop and Gjøsæter 2013). It reaches an average age of seven years (Hop, Welch et al. 1997). Males become mature at an age of two, whereas females first mature later, on average at an age of three years (Craig, Griffiths et al. 1982). Spawning takes place between December and March, peaking in January and February at a preferred spawning temperature of 1 – 2 °C (Hognestad 1966, Hognestad 1968). *B. saida* has a circumpolar distribution in waters with and without drifting sea ice (Ponomarenko 1968, Cohen, Inada et al. 1990). They feed on invertebrate species (Gastropoda, Larvacea, Chaetognatha), but mainly on Crustaceans like copepods (*Calanus finmarchicus*, *Calanus glacialis*) (Lønne and Gulliksen 1989). Polar cod itself is an important prey for various animals, such as birds, whales, and fish, including economically important fish species (Bradstreet 1982, Welch, Crawford et al. 1993). The core thermal habitat of *B. saida* is dependent on the life stage of the fish. The main thermal habitat of juveniles (0-group index) is 2.0 - 5.5 °C (Eriksen, Ingvaldsen et al. 2015), whereas adult fish (>age-1 fish) caught in the Canadian Beaufort Sea are found in regions of >0 °C between 20 and 1000 m depths (Majewski, Walkusz et al. 2016). Other studies showed that adult Polar cod inhabits the upper 20 m with temperatures above -1.5 °C and up to >2 °C as well as deeper waters (~130 m) with temperatures of -1.3 to -0.3 °C (Crawford and Jorgenson 1996, Crawford, Vagle et al. 2012). Although it was found that *B. saida* can cope short-term with temperatures up to 15.2 °C until cardiac arrhythmia sets in, the mean upper thermal limit that triggered cardiac arrhythmia is 12.4 °C, tested in a field study in Nunavut (Drost, Carmack et al. 2014). Drost et al. (2014) as well as other studies on both the cardiac mitochondrial function in response to environmental hypercapnia (Leo, Kunz et al. 2017) and the swimming behaviour under elevated temperatures (Schurmann and Christiansen 1994) showed that long-term exposure to increased temperatures decrease the fitness of Polar cod way before 12°C. Leo et al. (2017) showed that temperatures above 8 °C led to a decreased mitochondrial efficiency. Further experiments on the metabolism and performance of polar cod under ocean acidification and warming proved that the optimum growth performance under normocapnia was achieved at 6 °C, whereas the highest feed conversion efficiency was performed at 0 °C. Hypercapnia resulted in small losses in growth performance, but no significant temperature effect was observed (Kunz, Frickenhaus et al. 2016). In the study of Schurmann and Christiansen (1994), the preferred temperature for swimming activity was determined between 2.8 - 4.4 °C. This indicates that Polar cod has a confined ability to acclimate to rising temperatures.

1.2 Study area under climate change

Fjords on the west coast of Spitsbergen are influenced by hydrographically different water masses such as Atlantic-, Arctic-, brine-, and freshwater inputs. As they balance these diverse hydrographic influences, they are sensitive indicators for environmental changes (Nilsen, Cottier et al. 2008).

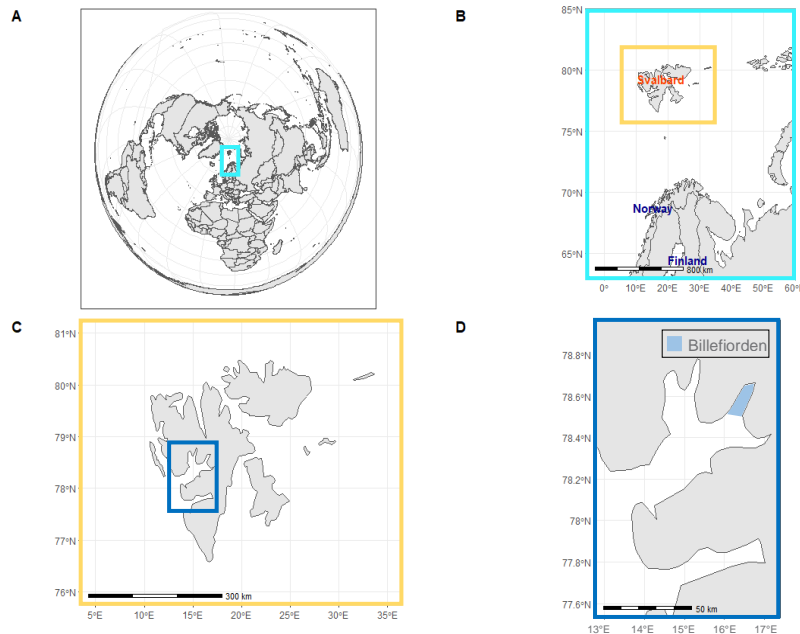


Figure 1 Study area Billefjorden (Svalbard archipelago). **A:** position of the Svalbard archipelago on a world map. **B:** position of the Svalbard archipelago in context of mainland. **C:** enlarged map of the Svalbard archipelago. **D:** exact position of Billefjorden.

The study area of this thesis is Billefjorden ($78^{\circ}34'59.99''$ N $16^{\circ}27'59.99''$ E), the innermost part of the Isfjorden, which is located at the west coast of the Svalbard archipelago (Figure 1). This two-silled fjord is 32 km long and 8-5 km broad, with an outer sill-depth of 70 m and an inner sill depth of 50 m (Figure 5). Its deepest area with approximately 200m is located about 4 km to the tidewater glacier Nordenskiöldbreen. On average, Billefjorden's main basin has a precipitous topography and is 160 m deep, with a maximum depth of 196 m at its northernmost edge. Szczucinski et al. (2009) found that the hydrography of the fjord is strictly layered during summer with little mixing between layers. They found surface water with a salinity lower than 34 and temperatures above 1°C , intermediate waters of around 34 psu, local fjord water with temperatures from -0.5 to 1°C and slightly higher salinity and below sill depth winter-cooled waters with salinity higher than 34.4 and temperatures lower than -0.5 . This unique hydrography distinguishes Billefjorden from other polar fjord-systems and is nowadays rarely found due to ongoing climate change (Figure 2).

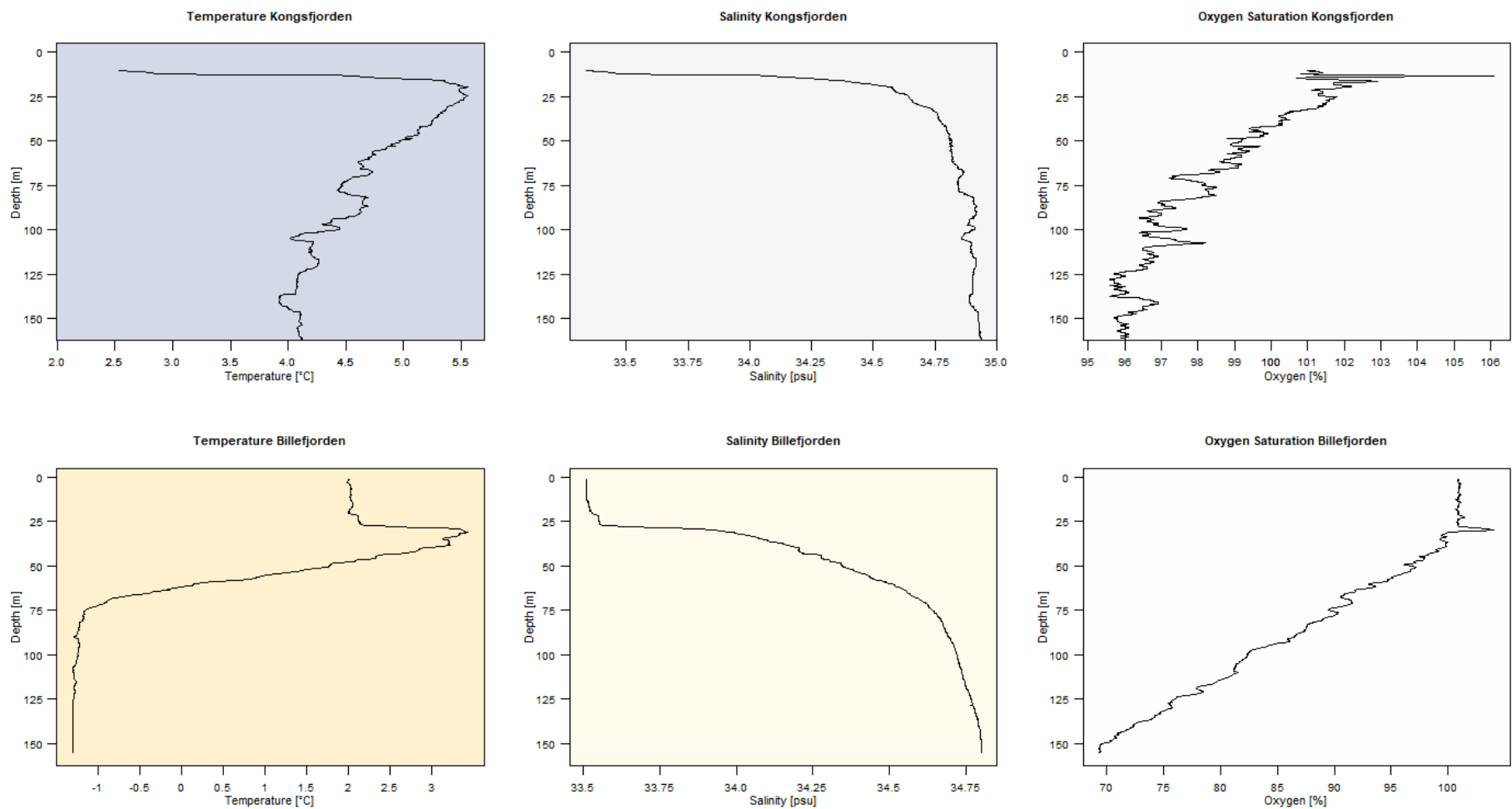


Figure 2 Comparison Kongsfjorden and Billefjorden. Upper row: depth profile of Kongsfjorden (04.10.2018) (11.6928°E, 78.9840°N), Lower row: depth profile of Billefjorden (06.10.2018) (16.4997°E, 78.5883°N), plots from left to right: temperature (°C), salinity (psu) and oxygen saturation (%) with increasing depth. (Data from: Mark and Wisotzki 2018).

Since industrialization the physicochemical conditions in the world's oceans changed dramatically. Under ongoing climate change, predicted values for the next hundred years are elevated atmospheric carbon dioxide (CO₂) pressure levels up to 1170 µatm; correspondingly the surface water temperatures will increase 2–3 °C, whereas the ocean surface pH will decrease 0.3 – 0.5 units by the year 2100 (Caldeira and Wickett 2005, Meinshausen, Smith et al. 2011, Pörtner, Karl et al. 2014). For the study area of this thesis, Svalbard, Førland et al. (2011) predicted an annual air temperature increase for the whole archipelago of maximum 8 °C and an increase in annual temperature of 4–6 °C in the region of Billefjorden (Figure 3). They moreover predicted winter maximum air temperatures for the year 2050 up to -2.5 °C and for 2100 up to 5 °C, maximum summer air temperatures in 2050 were prognosticated up to 8°C and up to 12 °C in 2100 (Figure 4). An average projected warming in the area of Billefjorden (measured for the Svalbard Airport/Longyearbyen area) from 1961–90 to 2071–2100 corresponded to an increase of 0.6 °C per decade for annual temperatures and a further increase of 0.9 °C per decade in winter is projected for 2071–2100 (Førland, Benestad et al. 2011).

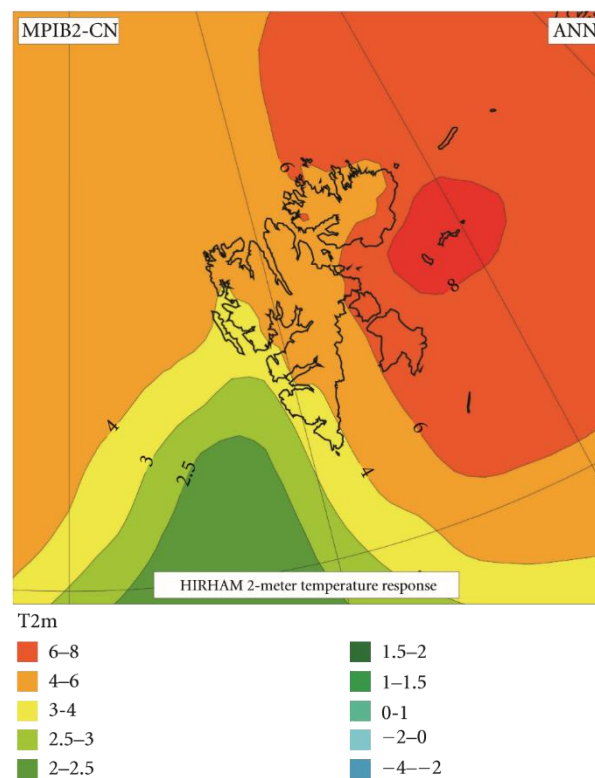


Figure 3 Projected changes from 1961–90 to 2071–2100 in mean annual temperature (°C) The RCM projections are based on MPIB2 (for acronyms, see Appendix Table 12; for weather stations used in the analysis, see Appendix Figure 21) (Førland, Benestad et al. 2011).

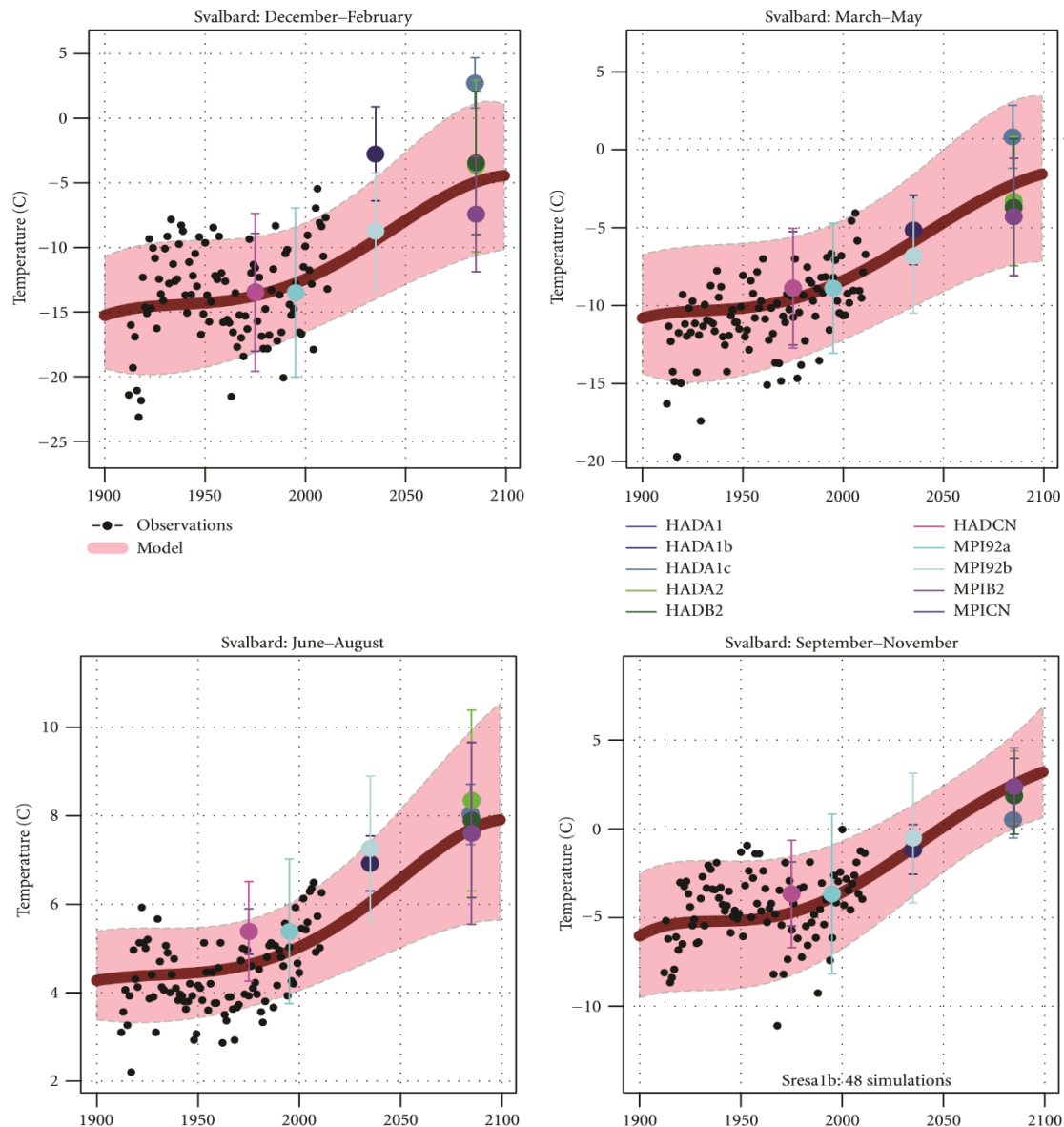


Figure 4 Temperature projections for Svalbard Airport/Longyearbyen: results from ESD and RCM downscalings for winter, spring, summer, and autumn. The hatched area (pink) shows 5 % and 95 % interval from ESD estimates, the black dots show observed values, and the thick line (red) show median (50 %) value for the ESD ensemble. The coloured symbols indicate the median value for the different runs with NorACIA-RCM, and the vertical lines show the 5- and 95-percentiles for the RCM runs. The RCM values are plotted on the central year in the respective time slices. (for acronyms, see Appendix Table 12; for weather stations used in the analysis, see Appendix Figure 21) (Førland, Benestad et al. 2011).

Furthermore, the oceans already lost 0.5 - 9 % of their oxygen solubility in cold regions (water temperature around 0 °C) and 0.3 - 5.2 % in tropical regions (40 °C) (Storch, Menzel et al. 2014). Additionally, increasing sea surface temperatures already decreased the sea ice by 49 % compared to the 1979-2000 baseline of $7.0 \times 10^6 \text{ km}^2$ (Kwok and Untersteiner 2011, Overland and Wang 2013). This sea ice loss can be observed in the fjord systems of the Svalbard archipelago, the study area of this thesis (Nilsen, Cottier et al. 2008, Szczuciński, Zajączkowski

et al. 2009). According to a business-as-usual greenhouse gas emission scenario (RCP8.5) (IPCC 2007), the Arctic is projected to be nearly ice-free in September before the year 2050 (Collins, Knutti et al. 2013). Not only the overall sea ice melting affects the Arctic ecosystem, warming of the western Svalbard fjords due to increasingly warm Atlantic water inflow also causes an overall temperature increase in the Arctic oceans interior (Polyakov, Timokhov et al. 2010). Besides declining sea surface salinities due to freshwater inflow, oxygen loss driven by lowered solubility of O₂ in warmer waters and decreased upper ocean stratification challenges marine organisms (Matear and Hirst 2003, Keeling, Körtzinger et al. 2009). Prominska et al. (2018) showed that winter cooled water is disappearing in warmer years completely out of some fjords, they proved that in Hornsund in the year 2012 winter cooled water was absent in this fjord and the water was dominated by local- and intermediate water. The warmer winter temperatures will reduce the sea ice formation in the fjords, thus no cold, dense, salty, and oxygen-rich water will be formed and the summer stratification will be intensified. As a result, the deep cold water layers do not receive oxygen-rich water and oxygen consumption extends over more than one season. This can lead to local hypoxia in the ground water layers of the protected fjords (Promińska, Falck et al. 2018). Another ecologically important effect of the temperature rise is the invasion of the boreal fish communities into the Arctic regions. Especially northward migration of predators such as *Gadus morhua* cause declines in Polar cod stocks (Simpson, Jennings et al. 2011, Renaud, Berge et al. 2012, Kjesbu, Bogstad et al. 2014).

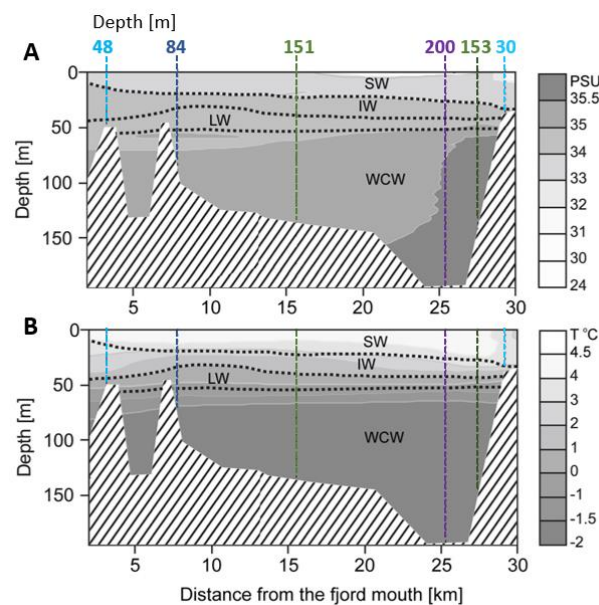


Figure 5 Hydrographic profile along the main axis of Billefjorden (August 2001) **A**: salinity, **B**: Water masses are marked by a dotted line, the shaded area marks land masses; SW – surface water, IW – intermediate water, LW – local water, WCW – winter-cooled water (modified after Szczuciński, Zajączkowski et al. 2009).

1.3 Physiological background

In aquatic ecosystems, dissolved oxygen is defined as the primary limiting factor and, together with temperature, dominates physiology as well as behaviour and defines the functional niche of all species (Claireaux and Lefrançois 2007, Pörtner and Knust 2007, Farrell and Richards 2009). For limiting concentrations of dissolved oxygen lower than 2.8 ml/L, the term “hypoxia” (\triangleq 39 % air saturation) is defined (Diaz and Rosenberg 1995). According to Henry’s Law (1903), increasing temperatures cause a reduction of oxygen solubility in the oceans. The oceans struggle under the expansion of (hypoxic) oxygen-depleted zones as a consequence of global warming. This oxygen loss affects the thermal tolerance of organisms as described in the concept of oxygen and capacity limited thermal tolerance (OCLTT) (Pörtner and Knust 2007, Pörtner and Lannig 2009, Pörtner, Bock et al. 2017). The concept of OCLTT explains that the capacity of the cardiorespiratory system to maintain the oxygen supply to the tissues sets the tolerance to low and high temperatures, and that these thermal limitations result from the capacity for oxygen supply to the organism in relation to oxygen demand (Pörtner and Knust 2007, Pörtner, Bock et al. 2017).

The “total aerobic excess capacity” is described as a key element for the overall performance of an animal within its thermal range. For the OCLTT concept, the aerobic metabolic scope (AS) is an important parameter to measure thermal stress and to approximate the aerobic performance balance (Pörtner, Bock et al. 2017). It is defined as the difference between minimum and maximum oxygen consumption rate [maximum metabolic rate (MMR) – standard metabolic rate (SMR)] (Pörtner and Lannig 2009). This assumes that there are positive correlations between the AS of an individual and its activity level (Baktoft, Jacobsen et al. 2016). Consequently, the AS is maximized in a defined temperature range to guarantee an optimal fitness (activity) level. The performance of an animal decreases as it is exposed to temperatures beyond or below the pejus temperature range (T_{pejus}). The AS will decrease until lethal temperatures are reached (Clark, Sandblom et al. 2013). Exhausting exercises are generally accepted to determine the MMR, therefore the critical swimming speed (U_{crit}) is experimentally detected, for example under decreasing oxygen (O_2) concentration (Brett 1964). Another method to describe the capacity of fish to maintain aerobic activities is the limiting oxygen level (LOL) curve (Figure 6) (Neill and Bryan 1991, Neill, Miller et al. 1994). The principle is similar to the OCLTT concept as the MMR decreases with decreasing oxygen concentrations until a threshold of critical oxygen concentration (P_{crit}) is reached. During the decrease of the MMR, organisms adjust their energy demand in reducing for example their

swimming activity (Domenici, Steffensen et al. 2000, Herbert and Steffensen 2005). When P_{crit} is reached the oxygen content in the water only allows short-term survival and anaerobic metabolism takes place. A further decline in oxygen leads to permanent anaerobic metabolism and a long-time exposure to these conditions to death, depending on the ability of the organism to decrease their SMR (Neill and Bryan 1991, Claireaux and Chabot 2016). The reaction of the organism to decreasing oxygen concentrations can be divided into two groups, either oxygen regulation or oxygen conformity. The metabolic rates of the oxygen regulators decrease in parallel with the decreasing oxygen concentration. As the oxygen concentration decreases, the metabolic rates of the oxygen regulators remain constant for a long time until P_{crit} is reached. When P_{crit} is reached, the oxygen regulators switch to oxygen conformers and their metabolic rates also start to decrease as the oxygen saturation continues to decrease below P_{crit} . (Ultsch, Jackson et al. 1981, Farrell and Richards 2009, Richards 2009).

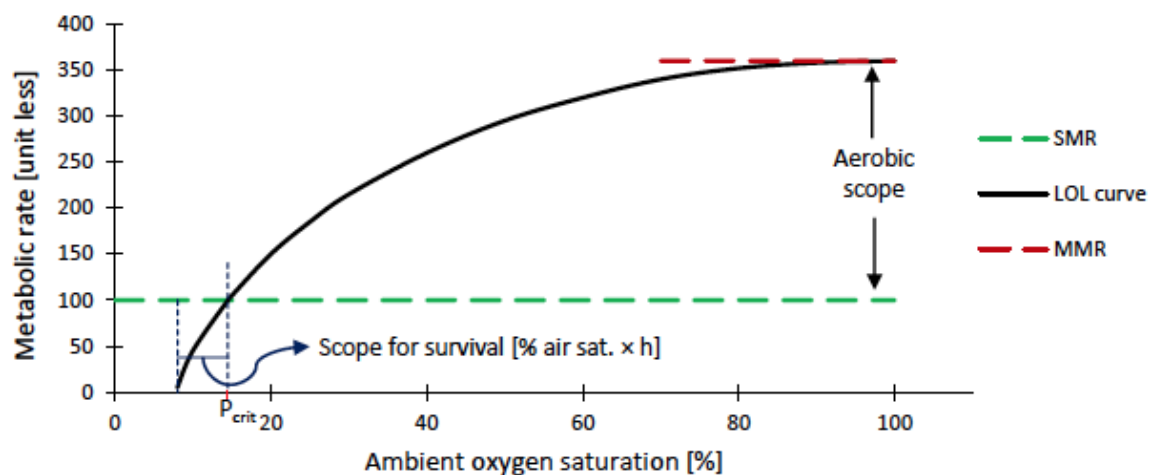


Figure 6 Limiting oxygen level (LOL) curve. The ambient oxygen saturation [%] influences the aerobic metabolic capacity of an idealized organism (modified after Claireaux and Chabot 2016). Shown are the maximum sustainable metabolic rate (MMR) (red dashed line) and standard metabolic rate (SMR) (green dashed line), the LOL curve (black), aerobic scope (distance between LOL curve and SMR) and the critical oxygen level (P_{crit}) (Neill and Bryan 1991, Claireaux and Chabot 2016).

To evaluate an animal's chance of survival under challenging environmental conditions, the SMR is a very important parameter, as it is defined as the minimal level of activity of organisms in total rest, without any muscular activity or even digestion. It only includes the minimal energy costs to sustain life (Krogh 1914).

2 Material and methods

B. saida were caught in October 2018 in Billefjord, Svalbard (Figure 1). They were caught on a research cruise with RV Heincke, Alfred Wegener Institute Helmholtz Centre for Polar and Marine Research, AWI (HE519), using a fish-lift connected to a pelagic trawl at 150m of depth. The water temperature was $-1.5\text{ }^{\circ}\text{C}$ and the oxygen concentration at 150m depth was 5.75 ml/l. The animals were directly transported to the laboratories of the Alfred Wegener Institute (AWI) in Bremerhaven. They were maintained in two flow-through tanks at normoxia and at an ambient temperature of $0.0 \pm 0.5\text{ }^{\circ}\text{C}$.

An experimental temperature of $2.5 \pm 1\text{ }^{\circ}\text{C}$ was chosen for respiration chambers and swim tunnel, according to the thermal window of *B. saida* (Hognestad 1968, Schurmann and Christiansen 1994, Eriksen, Ingvaldsen et al. 2015, Majewski, Walkusz et al. 2016). Experimental temperatures were maintained by aid of thermostatted rooms.

2.1 Fish tagging

Before the experiments were started a group of 30 fish between 17 and 23 cm were tagged with passive glass transponders (PIT tag, FDX-B, 7 x 1.35 mm, Loligo Systems Denmark). Before tagging, the fish were anesthetized in a solution of Tricaine methanesulfonate (MS-222) (1 g MS-222 per 8 L seawater). After approximately 3 min in the anaesthetic agent the completely motionless fish was measured (total and standard length, width and depth) and weighted. After that the PIT tag was inserted directly in front of the caudal fin using a disposable syringe needle implanter (Loligo Systems, Denmark) and read by a PIT reader, APR500 (Agrident GmbH, Germany) (Appendix: Table 7). All fish recovered in less than 10 min from this procedure and no later mortality due to tagging and handling stress occurred.

2.2 SMR and RMR measurements

The measurements were taken after Kunz et al. (2018). To ensure standard metabolism, the fish were transferred to the respiration chamber after the seventh day after feeding.

Two fully automated four chamber respirometry systems were used (Complete medium chamber system, Loligo Systems ApS, Denmark). As the ambient water oxygen saturation was measured using one of the oxygen meter ports only seven of the available eight respiration chambers were used in parallel in this experiment. The chambers were submerged in two identical basins, filled with 170 L, connected with U-pipes and one circulating pump. Besides three respiration chambers, one basin contained one oxygen and temperature sensor and the circulating pump, the other contained four chambers. Visual contact between the organisms was prohibited by an impermeable plastic wall between the chambers. For each respiration chamber the PO₂ was determined per second using fiber-optic mini sensors (optodes) placed in a probe vessel and connected to a four-channel oxygen meter (Loligo systems ApS, Denmark, Witrox 4 oxygen meter for mini sensors). The optodes were calibrated within the experimental set-up by flushing the basins with nitrogen to set for 0 % oxygen saturation and then calibrated for 100 % O₂ saturation in completely oxygen-saturated seawater. Due to calibration problems, some of the recorded oxygen values (100 – 5 %) had to be recalculated using a new 0 % calibration. Following a recalibration, the measurements at 10 and 5% were repeated with the correct 0% calibration (Troubleshooting is described under 2.4.9). The automated intermittent respirometry software, AuroResp (version 2.3.0, Loligo Systems ApS, Denmark) was used to acquire the oxygen saturation and temperature data within the chambers and control oxygen saturation in the basins and water flow through the chambers. Intermittent flow was chosen in this study. A measurement period of 30 min (only recirculation pumps working) was followed by a short waiting period of 30 sec and a 5 min long flushing phase (only flush pumps working).

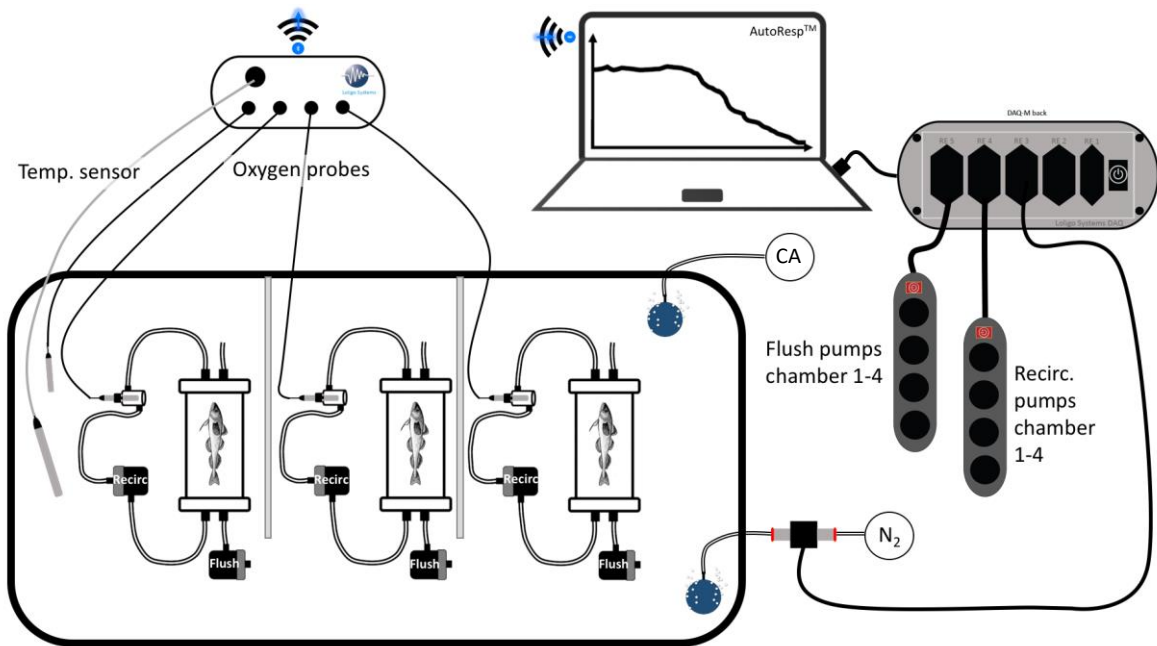


Figure 7 Schematic construction of the respirometry system. All respiration chambers are connected to one recirculation pump and one flush pump. Within the recirculating water, flow probe vessels are included where the oxygen probes are located. A four-channel oxygen meter (Loligo systems ApS, Denmark, Witrox 4 oxygen meter for mini sensors) detects the ambient oxygen in the chambers and basin as well as temperature, sending the data via Bluetooth to a computer with the software AutoResp version 2.3.0 (Loligo Systems ApS, Denmark). Compressed air (CA) together with nitrogen (N₂) create the desired oxygen concentration (100 - 5 % saturation). The data acquisition instrument (DAQ-M) controls the flush and recirculation pumps and the amount of nitrogen pumped into the water. DAQ-M is also connected to and controlled by a computer with the software AutoResp.

In the beginning of this study, eight different PO₂ steps were determined by a short initial experiment with seven individuals. After an initial oxygen saturation of 100 % was reached the flushing pumps were shut off, switching from intermitted flow to closed mode. The metabolic rate was calculated by the AutoResp software and graphically displayed. Consequently, the metabolic rate decreased with diminishing oxygen saturation and a possible P_{crit} (critical oxygen saturation) was determined. All fish performed well until 15-10 % oxygen saturation was reached. Compared to literature values for other Gadidae species the expected P_{crit} was assumed to be around 30 %. Therefore, the PO₂ steps for this experiment were chosen as follows to detect the exact P_{crit} for this species: 100, 75, 65, 50, 40, 30, 25, 20, 15, 10 and 5 % oxygen saturation. The desired oxygen concentration was maintained by constant gassing with compressed air and additional nitrogen, controlled by the AutoResp software. Each oxygen saturation was maintained for two days and two nights, containing approximately 80 measurement phases.

The rates of oxygen consumption were calculated after Boutilier et al. (Boutilier, Heming et al. 1984) and normalized after Steffensen et al. (Steffensen, Bushnell et al. 1994) (see below: 2.5. Data handling) using the statistical software “R” (package “FishResp” and “Mclust”).

All chambers were cleaned weekly. For this purpose, they were removed from the experimental setup, rinsed with tap water, wiped out and set up to dry for two days.

2.3 Swimming performance measurements

The metabolic rate and swimming performance of *B. saida* under hypoxia were recorded following a critical swimming speed (U_{crit}) protocol (Brett 1964). The following PO₂ steps for this experiment were selected: 100, 70, 60, 50, 40, 30, 25, 20, 15 and 10 % oxygen saturation. A sample size of six individuals was chosen for each PO₂ treatment.

A Brett-type swim tunnel respirometer of 5l (30 x 7,5 x 7,5 cm, Loligo Systems ApS, Denmark) was used to measure the swimming performance of *B. saida* (n=6 per treatment). To control the oxygen content and flushing phases, a DAQ-M instrument (Loligo Systems ApS, Denmark) was added to the system. The swim tunnel was submerged in a reservoir tank to maintain stable abiotic conditions within the chamber. The water velocity was regulated by a control unit regulating the engine controlling a propeller within the swim chamber (Loligo Systems ApS, Denmark). To calibrate the water velocity to voltage output from the control system, a flow sensor was used (Appendix: Figure 18). The PO₂ was determined using fiber optic mini sensors (optodes) connected to a four-channel oxygen meter (Loligo systems ApS, Denmark, Witrox 4 oxygen meter for mini sensors). The measurements were taken after Kunz et al. (2018). The desired oxygen concentration was maintained by constant gassing with compressed air and additional nitrogen, controlled by the AutoResp software.

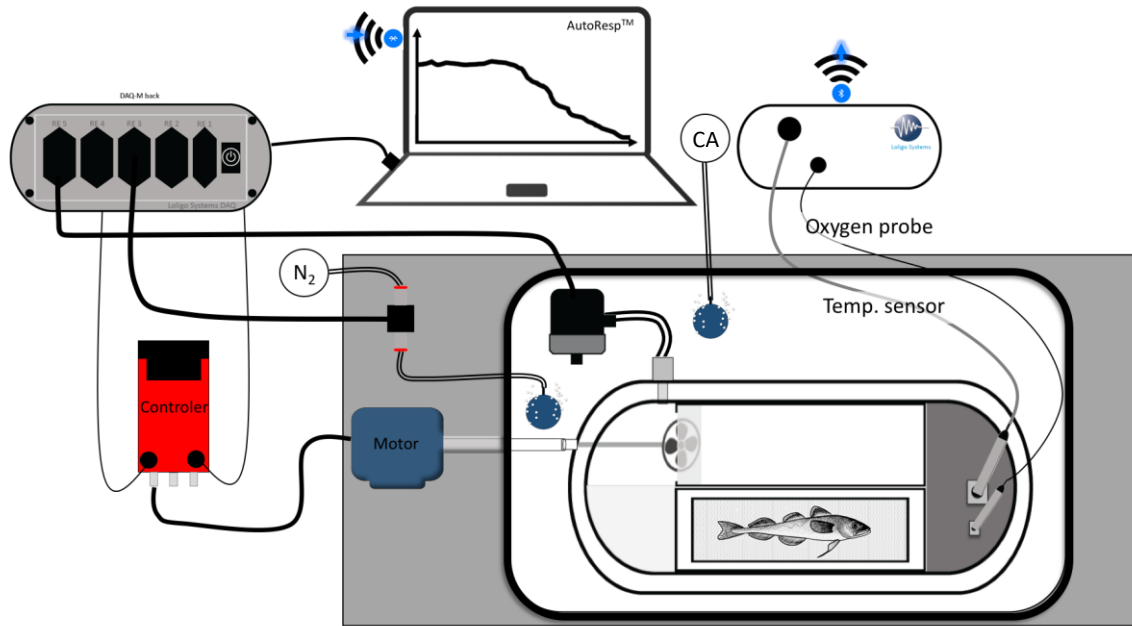


Figure 8 Schematic construction of the swim tunnel A four-channel oxygen meter (Loligo systems ApS, Denmark, Witrox 4 oxygen meter for mini sensors) detects the ambient oxygen in the swim tunnel as well as temperature, sending the data via Bluetooth to a computer with the software AutoResp version 2.2.0 (Loligo Systems ApS, Denmark). Compressed air (CA) together with nitrogen (N_2) create the desired oxygen concentration (100 – 10 % oxygen saturation). The data acquisition instrument (DAQ-M) controls the flush pump and the amount of nitrogen pumped into the water. DAQ-M is also connected to and controlled by a computer with the software AutoResp. A motor regulated by the controller drives the propeller, creating a laminar current within the swim tunnel. The fish is placed in the operation part of the tunnel.

Seven days after feeding the fish were transferred to the swim tunnel. In order to minimize air contact and possible oxygen stress, the fish were placed in the swim tunnel with a water-filled plastic bag. After an acclimatization period of 30 min the propeller was turned on and the fish were pre-conditioned to a water velocity of 1.2 BL (body length)/sec for 1 h and 25 min. Afterwards the velocity was increased to the first measurements velocity of 1.4 BL/sec for 5 min before the U_{crit} protocol started. This method was established to produce more robust swimming trials (Reidy, Kerr et al. 2000). A white plastic cover was used to minimize effects of disturbance. Subsequently, the U_{crit} protocol began at 1.4 BL/sec. The water velocity was increased by 0.15 BL/sec every 11 min. The flushing pump was switched on according to the velocity steps. A 30 second long flushing phase started after 11 min, when a specific velocity interval was over. After that a 30 second waiting period took place and then 10 min of measuring time followed to record oxygen consumption. To determine the gait-transition speed (U_{gait} : the speed at which the fish changes from strictly pectoral to pectoral-and-caudal swimming) (Heglund, Taylor et al. 1974, Heglund and Taylor 1988, Drucker and Jensen 1996)

the kick-and-glide swimming style (bursts) (Videler 1981) were documented. In kick-and-glide swimming, thrust generation is supplemented by anaerobic muscle contractions and mainly the white muscles are used. All bursts were counted and the corresponding time was documented. The water velocity was stepwise increased until the fish was exhausted. This was defined as the point at which a fish completely refused to swim and was inactive for more than three minutes. The critical swimming velocities (U_{crit}) of the fish were calculated as described by Brett (1964) (see: 2.4.7). After U_{crit} was reached the velocity was immediately decreased to the basic weaning velocity of 1.4 BL/sec for another 10 min the fish stayed in the swim tunnel. Afterwards the fish were set back into their collection tank. The maximum metabolic rate was determined under each oxygen saturation inside the swim tunnel, similar to the approach described for the respiration chambers above.

The swim tunnel was cleaned at the end of each day. For this purpose, the old water was removed from the swim tunnel, the tunnel was wiped dry and filled with fresh, pre-cooled sea water. All loose parts were also removed from the tunnel, flushed with tap water, wiped dry and returned to the swim tunnel.

2.4 Data handling

2.4.1 Oxygen consumption

The metabolic rates (M_{O_2}) were calculated using the R package “FishResp” on the basis of this equation:

$$M_{O_2} = \Delta P_{O_2} \cdot V \cdot \alpha \cdot M^{-1} \cdot \Delta t^{-1} \quad (1)$$

where ΔP_{O_2} is the change in water P_{O_2} (kPa), V is the volume of the respirometer (l) less the volume of the fish (l), α is the O_2 solubility coefficient after Boutilier et al. (1984), M is mass of fish (kg) and Δt is the elapsed time (h).

2.4.2 Normalized oxygen consumption

The M_{O_2} data was normalized using R package “FishResp” on the basis of this equation:

$$M_{O_2} = M_{O_{2(l)}} \cdot \left(\frac{BW}{100}\right)^{(1-A)} \quad (2)$$

with $M_{O_{2(100)}}$ is the oxygen consumption for a 100g fish, $M_{O_{2(l)}}$ is the oxygen consumption for a fish with a certain body weight (g) (BW), and A is the mass exponent describing relationship between metabolic rate and BW. As A, 0.8 will be used after Steffensen et al. (1994) and Holeton (1974).

2.4.3 Standard metabolic rate

The SMR was calculated after Chabot et al. (2016) in R, using the package “Mclust”. Only the data of the respiration chambers were used. Of these, only the data from the treatments 60 %, 70 % and 100 % were used for calculation, as in this oxygen range the metabolic rates of fish used to be stable. The lower 5 % of these data were removed as outliers, then a mean value of the remaining lower 15 % could be determined. This value was determined as SMR (Chabot, Steffensen et al. 2016).

2.4.4 Routine metabolic rates

The RMR was calculated in R. The metabolic rates recorded in the respiration chambers were grouped by treatments (5 - 100 % PO_2). For each fish within a PO_2 group, approximately 45 individual metabolic rates were calculated. After the lowest 5 % metabolic rates of each fish within a treatment were discarded as outliers, the mean value of the remaining lowest 15 % of each fish in the corresponding treatment was calculated and assumed as RMR of the respective fish. The mean value of all calculated RMRs in a treatment was calculated and taken as the RMR for that specific treatment. The standard deviation was calculated for each PO_2 group.

2.4.5 Maximum metabolic rates

Due to the short measuring time of maximum two hours, the number of measuring points per fish (between 3 and 10 individual metabolic rates) was too small to calculate the mean value of the highest 15% for each fish after the highest 5% were removed as outliers. Therefore, before determining the MMR, the highest 5% of all recorded metabolic rates of the swim tunnel experiment were removed as outliers. The remaining highest metabolic rate per fish was taken as MMR. The mean value of all individual MMRs in one treatment was calculated. The standard deviation was calculated for each PO₂ group.

2.4.6 Aerobic scope

The aerobic scope is defined as:

$$AS = MMR - SMR \quad (3)$$

In this study, only one RMR could be calculated for each fish and treatment. Since a state of complete immobility and dormancy of the organisms could not be achieved by the stay in the experimental set-up and therefore a RMR rather than a SMR has taken place. Therefore the AS was calculated as follows:

$$AS = MMR - RMR \quad (4)$$

All possible combinations between RMR (2.4.4) MMR (2.4.5) were calculated in R using the package “tidyr”, the differences between the newly paired RMR and MMR combinations within one PO₂ treatment (10 - 100 %) were calculated and a standard deviation was determined.

2.4.7 Critical swimming speed (U_{crit}) after Brett (1964)

The critical swimming speed was adjusted as:

$$U_{crit} = U_{max} + \frac{vT}{t} \quad (5)$$

In this equation U_{max} is the highest velocity (v) perpetuated for a complete time interval (t) and T is the time spent at the given velocity leading to exhaustion of the fish.

2.4.8 Gait transition speed (U_{gait})

The critical swimming speed was adjusted as:

$$U_{\text{gait}} = U_{\text{max}} + \frac{vT}{t} \quad (6)$$

In this equation U_{max} is the highest velocity (v) perpetuated for a complete time interval (t) without bursting and T is the time spent at the given velocity leading to bursting of the fish.

2.4.9 Troubleshooting

Due to calibration problems (initial drift of 0 % calibration), some of the recorded oxygen values (100-5 %) had to be recalculated using a new 0 % calibration. After a new 0 % calibration was performed these calibration values were used to recalculate the recorded oxygen concentrations with the PreSens Oxygen Calculator (version 3.1.1, PreSens Precision Sensing GmbH, Germany). Therefore, the data had to be converted to an excel-file written with PreSens Measurement Studio 2 (version 3.0.1, PreSens Precision Sensing GmbH, Germany). This program detects all calibration coefficients of an optical oxygen sensor, needed to recalculate the data, automatically. In PreSens Measurement Studio 2 short measurement files with the identical oxygen optodes used in the main experiment were performed. After that the raw data from AutoResp were inserted into this data file. All values as partial pressure, salinity and temperature were transferred to the new file as well. Afterwards this file could be recalculated with the calculator. For this purpose the new calibration values for the corresponding optode had to be entered in the software. The calculator returned a new file with corrected values which could be used to calculate the correct metabolic rate (using the R package “FishResp”).

2.4.10 Statistical analysis

The normal distribution of the data was determined using the Shapiro-Wilk test or the Kruskal-Wallis test. The homoscedasticity was evaluated with the Levene test. The differences between PO_2 treatments were evaluated with a one-way (respirometry chambers, burst counts and swimming time) or two-way ANOVA (swim tunnel) followed by Tukey’s test for mean value comparison. Furthermore, the influence of body weight, body length, temperature and water velocity were examined. The level of statistical significance was set at $p < 0.05$ for all statistical tests. All statistical tests were performed with R 3.6.1.

3 Results

3.1 Mortality

Within the experimental setups, Polar cod mortality occurred solely at the lowest PO₂ treatment in respiration chambers. Two Polar cod died during the acclimation phase, the first night after they were placed in the chambers. Another four individuals died in the holding aquarium, independent of the handling stress.

3.2 Respiration measurements

All measurements were significantly influenced by individual body weight ($p_{\text{RMR}} < 0.0001$, $p_{\text{MMR}} = 0.0039$). A significant temperature effect only occurred in the respiration chambers ($p < 0.0001$). The temperature differed between 2.2 and 3.2 °C, with a mean temperature of 2.68 ± 0.25 °C. The MMR was significantly influenced ($p = 0.0082$) by individual body lengths as well. The swim tunnel measurements were maintained at a temperature of 1.23 ± 0.34 °C

3.2.1 Standard metabolic rate

The SMR of *B. saida* was calculated after Chabot et al. (2016) (see 2.4.3) using the lower 15 % quantile of the metabolic rates recorded under 60-100% oxygen saturation in respiration chambers. This includes metabolic rates of 29 individuals. The calculated SMR of Polar cod was $0.44 \mu\text{mol O}_2/\text{g}\cdot\text{h}$.

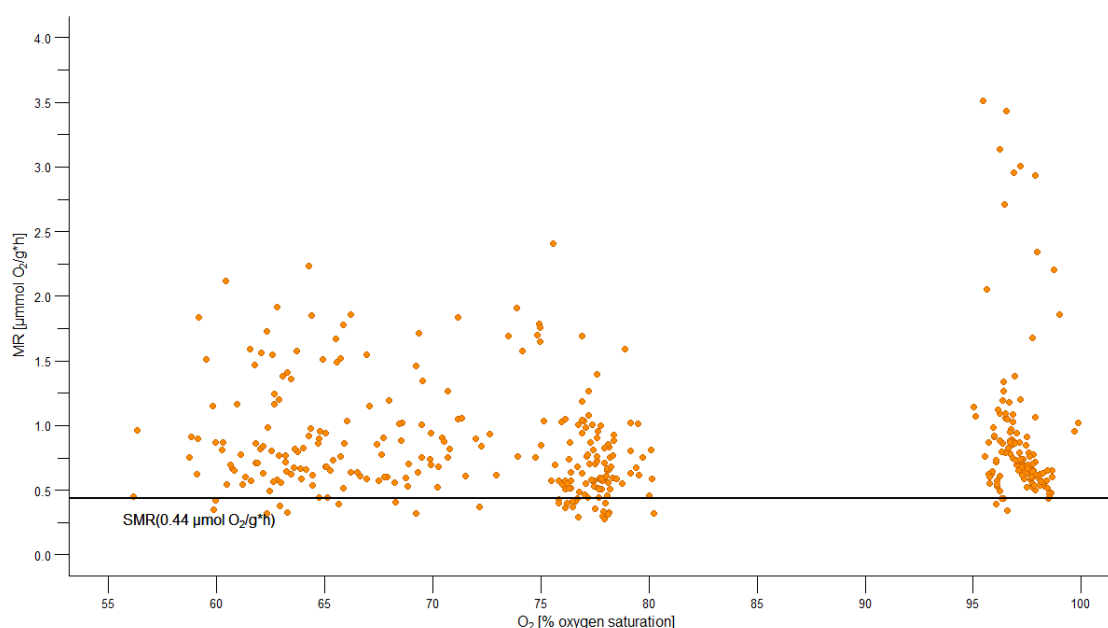


Figure 9 Standard metabolic rate (SMR). Shown are the metabolic rates ((MR) in $\mu\text{mol O}_2/\text{g}\cdot\text{h}$) (orange circles) recorded at 56 - 100 % PO₂. The SMR ($0.44\mu\text{mol O}_2/\text{g}\cdot\text{h}$; black line) was calculated as described under point 2.4.3 using the R package “Mclust” after Chabot et al. (2016).

3.2.2 Standard and routine metabolic rate

After fish were placed in the respiration chambers their oxygen consumption declined during the first 36 h, reaching a steady level afterwards. Therefore, the measurements recorded within the second night were used in this study, when fish had been in the respirometer setups for an average of 36 h.

The metabolic rates were significantly dependent on PO_2 ($p = <2e-16$). The calculated RMR (Figure 10, Table 1) remained on a similar level between 100 and 45 % PO_2 (max: 0.97 ± 0.81 , min: $0.53 \pm 0.13 \mu\text{mol O}_2/\text{g}\cdot\text{h}$), below which oxygen consumption slightly increased between 45 and 35 % oxygen saturation up to $1.78 \pm 0.35 \mu\text{mol O}_2/\text{g}\cdot\text{h}$ ($p < 0.0001$). From 35 to 20 % oxygen saturation the metabolic rate decreased constantly down to $1.06 \pm 0.31 \mu\text{mol O}_2/\text{g}\cdot\text{h}$ ($p < 0.0001$). Between 20 and 5 % oxygen saturation the oxygen consumption remained stable and did not decrease below the SMR level. The minimum routine metabolic rate reached in this experiment was $0.86 \pm 0.14 \mu\text{mol O}_2/\text{g}\cdot\text{h}$ at 10.97 ± 0.92 % PO_2 .

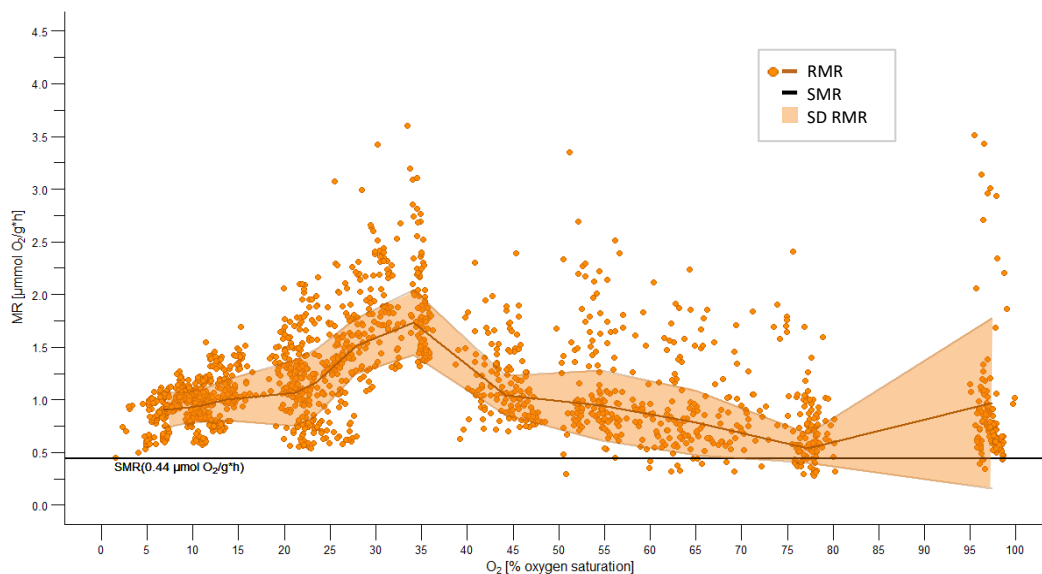


Figure 10 Routine metabolic rate (RMR). Shown are the metabolic rates ((MR) in $\mu\text{mol O}_2/\text{g}\cdot\text{h}$) (orange circles) (86 experimental runs representing 1887 single metabolic rate data points of 30 individuals) performed between 5 and 100 % PO_2 in respiration chambers. The RMR (dark orange line, with SD (light orange area)) was calculated as described under point 2.4.4. Black line: standard metabolic rate (SMR; $0.44 \mu\text{mol O}_2/\text{g}\cdot\text{h}$).

Table 1 P-values of TukeyHSD, RMR. Comparison of all treatments and the corresponding metabolic rates from respirometry chambers. Significant p-values are printed in bold type. Treatments 10 and 5% PO₂ have been repeated due to recalibration of the oxygen optodes.

Treatments	100%	70%	60%	50%	40%	30%	25%	20%	15%	10(2)%	10%	5%	5(2)%
100%													
70%	0.014680429												
60%	1	0.024593444											
50%	1.01E-05	2.26E-11	2.04E-06										
40%	3.45E-06	2.26E-11	6.59E-07	0.9999999998									
30%	2.25E-11	2.25E-11	2.25E-11	2.25E-11	2.25E-11								
25%	2.25E-11	2.25E-11	2.25E-11	2.25E-11	2.25E-11	1.13E-08							
20%	7.65E-09	2.26E-11	1.02E-09	0.987165455	0.998328926	2.25E-11	2.26E-11						
15%	0.000464578	2.27E-11	0.000126054	0.999941846	0.998951009	2.25E-11	2.25E-11	0.723453982					
10(2)%	0.001192183	2.29E-11	0.00034953	0.99916719	0.993191858	2.25E-11	2.25E-11	0.569527547	1				
10%	0.999999049	0.063349146	0.999999997	3.06E-07	9.43E-08	2.25E-11	2.25E-11	1.26E-10	2.48E-05	7.40E-05			
5%	0.964941963	4.79E-06	0.891995795	0.001134415	0.000420242	2.25E-11	2.25E-11	1.33E-06	0.029019712	0.060583148	0.6988863		
5(2)%	0.999998877	0.024681127	0.999999998	1.45E-08	3.91E-09	2.25E-11	2.25E-11	2.39E-11	2.66E-06	9.58E-06	1	0.572368959	

3.2.3 Standard and maximum metabolic rate

Following an acclimatisation phase of two hours to basic water velocity and the environment, 60 experimental runs recorded the metabolic rates of 30 Polar cod, some of which were used repeatedly. The metabolic rate was significantly influenced by PO_2 ($p < 0.0001$) and water velocity ($p < 0.0001$) (all p-values in Table 2). The MMR (blue curve, Figure 11) stayed on a comparable level between 100 and 45 % oxygen saturation (max: 4.39 ± 0.56 , min: 3.72 ± 1.13 $\mu\text{mol O}_2/\text{g}\cdot\text{h}$), with a small decline at 71.53 ± 1.84 % oxygen saturation down to 3.27 ± 0.53 $\mu\text{mol O}_2/\text{g}\cdot\text{h}$. Beginning with 31.28 ± 1.52 % oxygen saturation the metabolic rate (3.68 ± 0.55 $\mu\text{mol O}_2/\text{g}\cdot\text{h}$) started to follow an oxyconforming pattern and decreased with decreasing oxygen saturation. Between 30 and 20 % oxygen saturation, respiration rate followed an exponential decline. After 20% oxygen saturation a linear decrease in oxygen consumption occurred until a metabolic rate of 1.38 ± 0.12 $\mu\text{mol O}_2/\text{g}\cdot\text{h}$ was reached at 10.92 ± 1.50 % oxygen saturation.

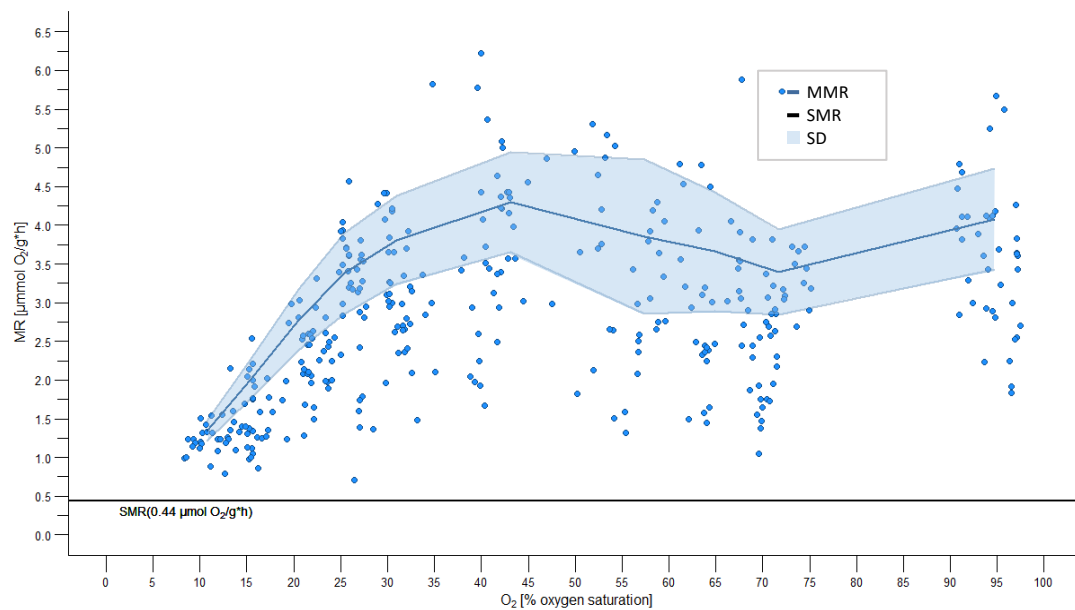


Figure 11 Maximum metabolic rate (MMR). Shown are the metabolic rates ((MR) in $\mu\text{mol O}_2/\text{g}\cdot\text{h}$) (blue circles) (60 experimental runs representing 361 single metabolic rate data points of 30 individuals) performed between 10 and 100 % PO_2 in the swim tunnel. The MMR (dark blue line, with SD (light blue area)) was calculated as described under point 2.4.5. Black line: standard metabolic rate (SMR; $0.44 \mu\text{mol O}_2/\text{g}\cdot\text{h}$).

Table 2 P-values of TukeyHSD, MMR and PO₂. Comparison of all treatments and the corresponding metabolic rates from swim tunnel. Significant p-values are printed in bold type.

Treatments	100%	70%	60%	50%	40%	30%	25%	20%	15%	10%
100%										
70%	0.00024255									
60%	0.24583604	0.56790737								
50%	0.54712282	0.22449605	0.99996069							
40%	0.99339004	1.54E-06	0.01533482	0.06498307						
30%	0.06607839	0.68494223	0.99999933	0.99675999	0.00139251					
25%	0.04170468	0.92347713	0.99970074	0.97323801	0.00101209	0.99999703				
20%	4.32E-08	0.8218915	0.00922803	0.00099827	6.22E-11	0.01097082	0.06656189			
15%	< 2.33E-12	1.48E-06	2.33E-12	< 2.33E-12	< 2.33E-12	< 2.33E-12	2.01E-10	0.00345114		
10%	< 2.33E-12	1.58E-08	< 2.33E-12	6.96E-05	0.97720314					

3.2.4 Standard-, routine-, maximum metabolic rate and aerobic scope

The aerobic scope displayed in figures 12 and 13 significantly decreased with decreasing oxygen saturation ($p < 0.0001$). Aerobic scope decreased stepwise and three significantly different levels could be determined relative to PO₂ ($p < 0.0001$). Within the oxygen range from 96.00 ± 2.45 % to 43.62 ± 1.69 %, aerobic scope was 3.02 ± 0.25 $\mu\text{mol O}_2/\text{g}\cdot\text{h}$. In comparison the aerobic scope decreased in the second group (from 32.52 ± 0.85 to 20.84 ± 0.45 % oxygen saturation) to 1.93 ± 0.004 $\mu\text{mol O}_2/\text{g}\cdot\text{h}$. In the lowest group of oxygen concentrations from 14.48 ± 0.25 % to 10.87 ± 0.19 %, aerobic scope was also lowest with 0.71 ± 0.14 $\mu\text{mol O}_2/\text{g}\cdot\text{h}$. The on average highest value for the aerobic scope with 3.40 ± 0.60 $\mu\text{mol O}_2/\text{g}\cdot\text{h}$ was recorded at 43.62 ± 1.69 % oxygen saturation. The difference between the highest and lowest value was 2.84 $\mu\text{mol O}_2/\text{g}\cdot\text{h}$.

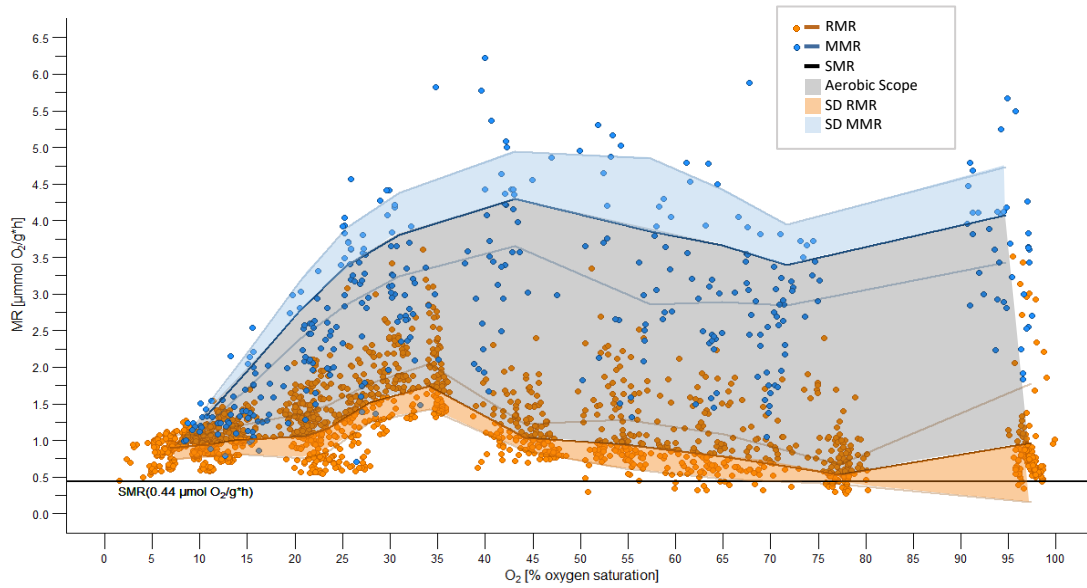


Figure 12 Routine- (RMR), maximum- (MMR) and standard metabolic rate (SMR) of 148 single measurements with a total of 30 multiple used individuals. Metabolic rates ((MR) in $\mu\text{mol O}_2/\text{g}\cdot\text{h}$) at the different oxygen saturation (%). Data from both, swim tunnel and respiration chamber, experiments. In blue: metabolic rate of 60 individuals recorded during swim tunnel experiments. In orange: metabolic rate of 86 individuals recorded during measurements in respirometry chambers. Upper blue line: maximum metabolic rate (swimming tunnel; calculated as described in 2.4.5). Lower dark orange line: routine metabolic rate (respiration chambers; calculated as described in 2.4.4). Black line: SMR (respiration chambers; calculated as described in 2.4.3). Grey shaded area: aerobic scope (difference between MMR and RMR).

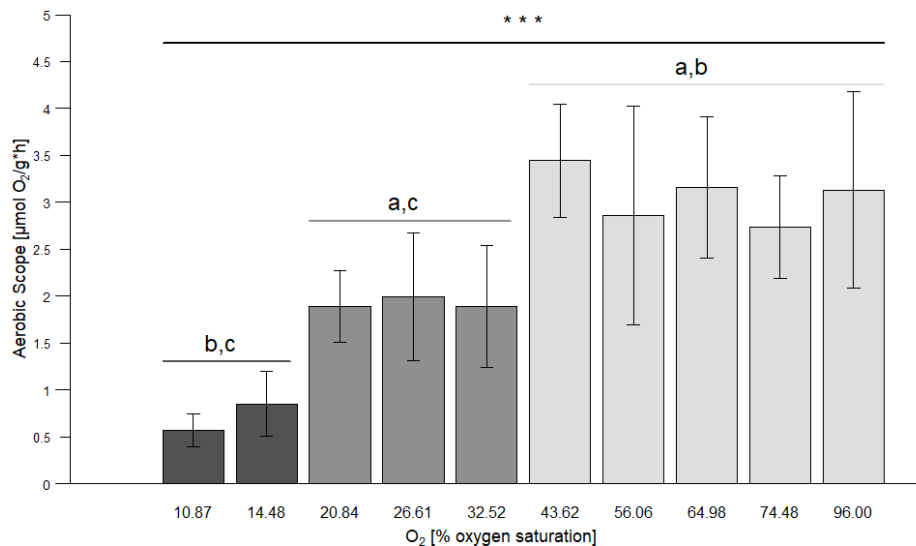


Figure 13 Aerobic scope. Bars represent the mean aerobic scope of Polar cod at ten different oxygen saturations (treatments). The different grey shadings represent three significantly different levels of AS. Aerobic scope was calculated as described in 2.4.6. Error bars depict standard deviation. Asterisks: significant difference between the three decreasing levels of AS (***, or a, b, c for the three steps), all p-values are lower than 0.0001.

3.2.5 LOL curve and P_{crit}

For *B. saida* a P_{crit} of 4.81 % oxygen saturation ($\cong 0.71$ mg O₂/l) was determined (Figure 14). Only the intersection point of the MMR and SMR regression line could be used for P_{crit} calculations, since the regression line calculated for the RMR had no intersection point with the SMR regression line (Appendix Figure 19)

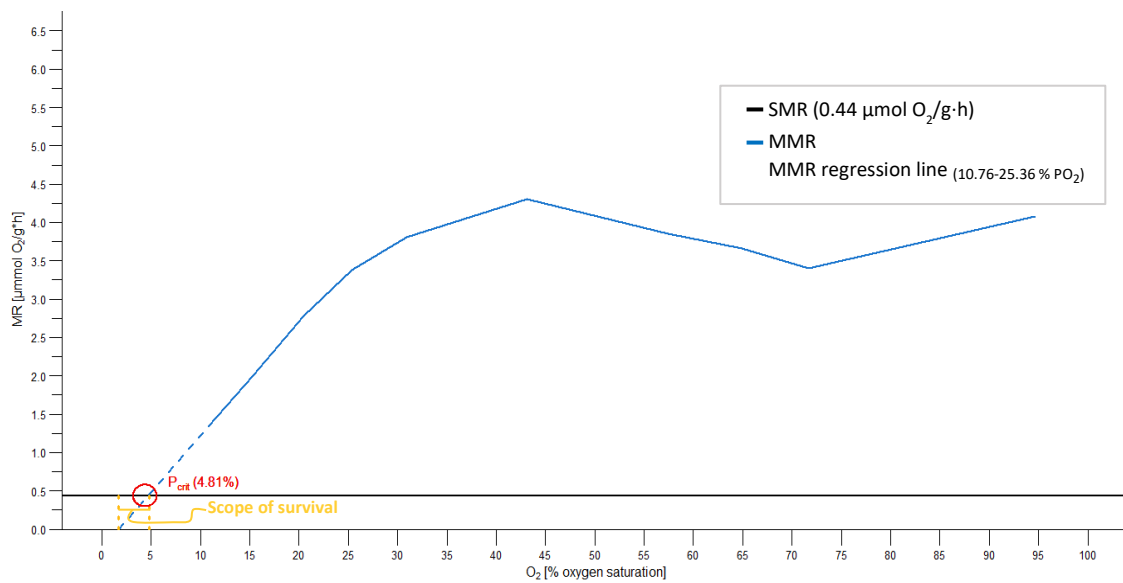


Figure 14 Limiting oxygen level (LOL) curve after Claireaux and Chabot (2016). Shown are the maximum metabolic rate (MMR; blue line) and standard metabolic rate (SMR; black line), MMR regression line (dashed blue line; polynomial regression of the MMR between 10.77 and 25.36 % PO₂ ($y = 1E-06x^2 + 0.0002x - 0.0005$; $R^2 = 0.9994$)), the critical oxygen level (P_{crit} (4.81 %), red circle, intersection between MMR regression line and SMR) and the scope of survival (between 1.71 and 4.81 % PO₂).

3.3 Swimming performance

Following an acclimatisation phase of two hours to basic water velocity and the environment, 60 experimental runs recorded the metabolic rates of 30 Polar cod, some of which were used in several runs. The metabolic rate was significantly influenced by PO_2 ($p < 0.0001$) and water velocity ($p < 0.0001$).

3.3.1 MR at different water velocities

In this study, the metabolic rate increased significantly with increasing water velocities ($p < 0.0001$) (Figure 15, Table 3) ($p < 0.0001$). The highest metabolic rates occurred at 2.60 BL/sec with an average metabolic rate of $4.94 \pm 0.80 \mu\text{mol O}_2/\text{g}\cdot\text{h}$. The sample size decreased with increasing water velocities, because most fish refused to swim at high water velocities. *B. saida* began to refuse swimming at 1.85 BL/sec. The incomplete sample size ($n=59$) at 1.40 and 1.55 BL/sec is due to measurement disturbances of the oxygen optodes. It was not possible to fit a meaningful regression line for slope calculations into the oxygen consumption data ($R^2 < 0.4$)

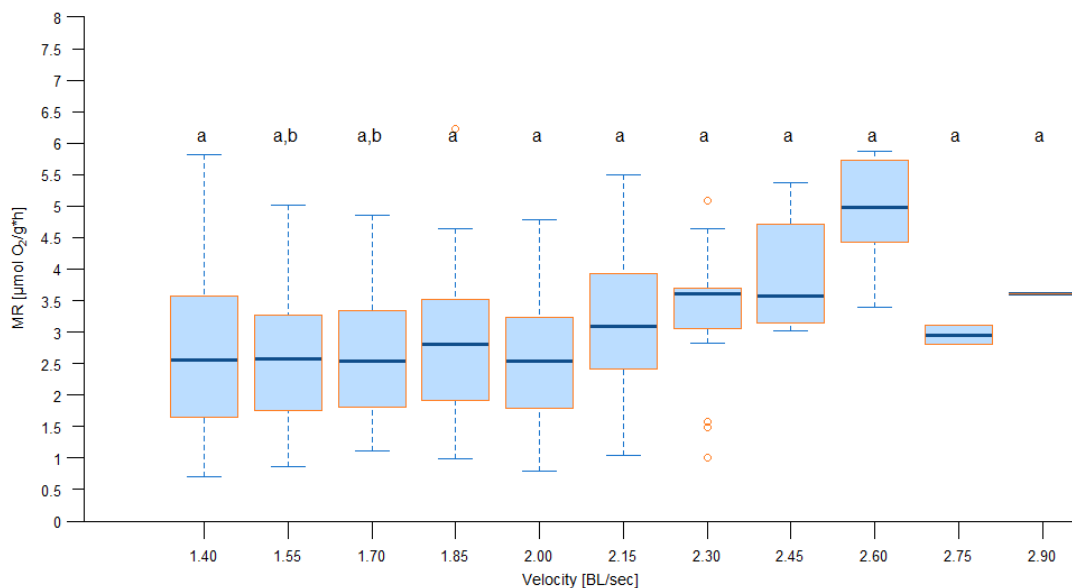


Figure 15 Metabolic rates over increasing water velocities. Boxplots (with median and outliers) show the results of the swim tunnel measurements. Displayed are the MR [$\mu\text{mol O}_2/\text{g}\cdot\text{h}$] during increasing water velocities [BL/sec]. Letters indicate results of Tukey honest significance test between Velocity treatments. Significant differences are represented by different letters, the corresponding p-values can be found in Table 3. (n per velocity: 1.40=59, 1.55=59, 1.70=60, 1.85=56, 2.00=45, 2.15=38, 2.30=21, 2.45=12, 2.60=8, 2.75=2, 2.90=1).

Table 3 P-values of TukeyHSD, MMR and velocity. Comparison of all velocity treatments and the corresponding metabolic rates from swim tunnel. Significant p-values are printed in bold type.

Treatments (Velocity [BL/sec])	1.4	1.55	1.7	1.85	2	2.15	2.3	2.45	2.6	2.75	2.9
1.4											
1.55	2.65E-07										
1.7	2.89E-07	2.46E-02									
1.85	9.60E-07	8.92E-02	6.11E-01								
2	1.14E-06	9.41E-02	6.84E-01	9.97E-01							
2.15	3.94E-04	2.28E-01	9.53E-01	9.98E-01	1.00E+00						
2.3	2.64E-03	3.65E-01	9.56E-01	9.98E-01	1.00E+00	1.00E+00					
2.45	2.83E-03	3.98E-01	9.65E-01	9.99E-01	1.00E+00	1.00E+00	1.00E+00				
2.6	6.90E-03	4.37E-01	9.86E-01	9.99E-01	1.00E+00	1.00E+00	1.00E+00	1.00E+00			
2.75	4.41E-06	1.85E-01	7.70E-01	9.98E-01	1.00E+00	1.00E+00	1.00E+00	1.00E+00	1.00E+00		
2.9	8.72E-03	4.48E-01	9.89E-01	1.00E+00							

3.3.2 Gait transition speed U_{gait}

An interaction between U_{gait} and PO_2 level was not found ($p = 0.86$). Nonetheless the total occurrence of bursts was reduced under insufficient oxygen supply (Figure 16, Table 4). Under treatment 20 % (21.70 ± 0.57 % oxygen saturation) only three individuals displayed burst swim behaviour at all. The remaining three Polar cod stopped swimming without detectable burst actions before. In comparison only one Polar cod remained bursting under treatment 10 % (10.67 % oxygen saturation and $U_{\text{gait}} = 1.87$ BL/sec). Looking at the median of the different oxygen treatments U_{gait} remained at a constant level between 100 and 30 % oxygen saturation (2.25 BL/sec). Following this constant trend, the gait transition speed decreased parallel to the total number of fish which remained bursting ($p = 0.054$). Under the treatments 100, 70, 60, 50 and 30 % PO_2 all fish remained bursting. Only five fish showed kick-and-glide swimming at 42.02 ± 3.18 % PO_2 , three fish at 21.07 ± 1.60 % PO_2 , two at 15.52 ± 1.26 % PO_2 and only one at 10.91 % PO_2 . Additionally, the burst activity, meaning the total number of bursts ($p = 0.025$) and the number of bursts per minute ($p = 0.054$) decreased significantly with decreasing PO_2 (burst data: Table 4). The maximum number of 14.56 ± 9.33 bursts per minute was achieved at 31.28 ± 1.52 % PO_2 . From this peak on the number of bursts per minute started to decrease. At 21.07 ± 1.60 % PO_2 burst occurrence already decreased to 3.24 ± 4.34 bursts per minute (raw data burst performance: Appendix Table 9).

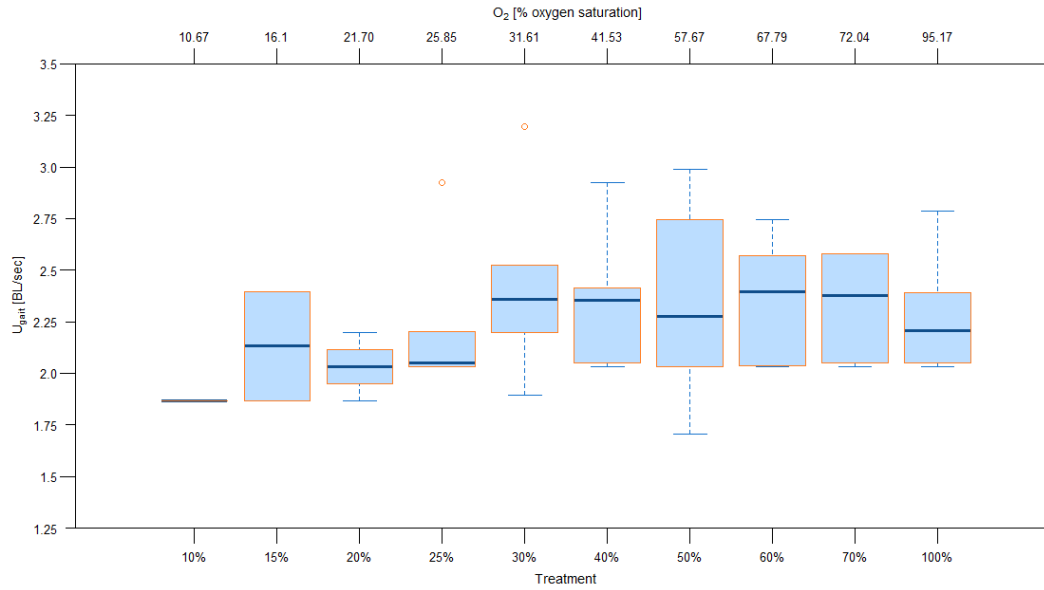


Figure 16 Gait transition speed (U_{gait}) over increasing oxygen concentrations. Comparison of U_{gait} (BL/sec) at different oxygen levels (n per treatment: 10=1, 15=2, 20=3, 25=6, 30=6, 40=5, 50=6, 60=6, 70=6, 100=6). No significance between PO_2 treatments was observed.

Table 4 Burst activity. Mean total number of bursts (with standard deviation, SD) and mean bursts per minute (with SD) of all fish ordered by PO_2 treatments.

Treatment	Mean total number of bursts	SD	Mean bursts per min	SD
100%	146.17	211.93	12.61	9.39
70%	22.33	21.68	6.23	3.39
60%	18.83	32.87	7.48	7.11
50%	36.33	54.97	13.55	17.42
40%	43.33	35.86	10.42	9.67
30%	47.50	38.04	14.56	9.33
25%	14.83	12.85	10.11	8.96
20%	27.50	42.99	3.24	4.34
15%	5.50	8.04	2.34	3.50
10%	0.83	1.86	1.14	2.54

3.3.3 Critical swimming speed (U_{crit})

U_{crit} (Figure 17) revealed a significant oxygen effect ($p=0.044$). Although U_{crit} remained relatively high throughout all treatments, values under the 10% treatment can be assumed as significantly lower compared to the 70% PO_2 treatment ($p=0.031$) (Table 2). The fish were able to swim at high water velocities under hypoxia, yet the overall active swimming phases of all fish significantly decreased, with a little increase between 57.52 ± 3.93 and 21.07 ± 1.60 % PO_2 from 41.3 ± 21.66 to 67.31 ± 4.74 % active swimming, with decreasing oxygen saturation ($p=0.017$) (swimming data: Table 5). The maximum active swimming duration of 80.93 ± 10.91 % was achieved at 94.50 ± 2.22 % PO_2 which was more than twice as high as the swimming participation at 10.92 ± 1.50 % PO_2 (31.35 ± 18.50 % active swimming). All fish had to rest for longer periods of time, which differed from U_{crit} in that all fish interrupted their inactive phases with short swims. Therefore, the maximum inactivity time of three minutes, which was set as an indication of U_{crit} in this study, was not reached. This indicated that swimming was still possible at the specific water speed and U_{crit} had not yet been reached (raw data swimming performance: Appendix Table 9 and Table 10).

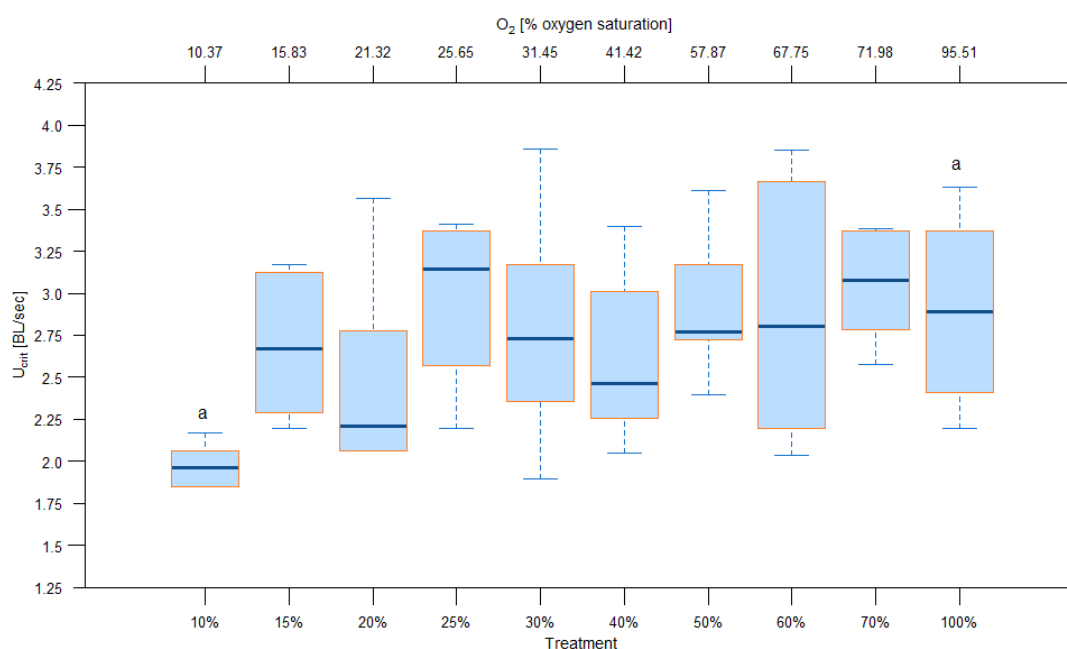


Figure 17 Critical swimming speed (U_{crit}) over increasing oxygen concentrations. Comparison of U_{crit} (BL/sec) at different oxygen levels ($n:6$ per treatment). Letters indicate results of Tukey honest significance test between PO_2 treatments ($p=0.031$). All other p -values can be found in Table 6.

Table 5 **Swimming activity.** Mean percentage of active (with standard deviation, SD) and inactive phases (with SD) and the mean of the total swim time [min] (with SD) during the swim tunnel experiments ordered by PO₂ treatments.

Treatment	Mean aktiv [%]	SD	Mean inaktiv [%]	SD	Mean swimming time [min]	SD
100%	80.93	10.91	19.07	10.91	53.01	16.52
70%	68.72	10.71	31.28	10.71	38.79	9.75
60%	40.46	10.71	59.54	10.71	27.37	14.33
50%	41.30	21.66	58.70	21.66	31.16	22.99
40%	56.90	16.27	45.72	16.27	47.82	22.27
30%	54.28	22.83	45.72	22.83	41.28	20.20
25%	59.20	26.34	40.80	26.34	48.72	27.34
20%	67.31	4.74	32.69	4.74	39.68	4.65
15%	42.66	17.02	57.34	17.02	23.44	10.80
10%	31.35	18.50	68.65	18.50	12.38	8.82

Table 6 **P-values of TukeyHSD, U_{crit} and PO₂.** Comparison of all treatments and the corresponding metabolic rates from swim tunnel. Significant p-values are printed in bold type.

Treatments	100%	70%	60%	50%	40%	30%	25%	20%	15%
100%									
70%	0.99997385								
60%	1	0.99996537							
50%	1	0.99998488	1						
40%	0.99336437	0.90914011	0.99413433	0.99173138					
30%	0.99999828	0.9977153	0.99999886	0.9999965	0.99981039				
25%	0.99999993	0.99999995	0.99999987	0.99999998	0.96866234	0.99984146			
20%	0.93209437	0.70430371	0.93661061	0.92320261	0.99999361	0.989968	0.83740843		
15%	0.99947153	0.97384511	0.99956339	0.99925864	0.99999983	0.99999872	0.9945092	0.99954574	
10%	0.10241997	0.03078164	0.10628039	0.09559762	0.56438654	0.21603512	0.05684301	0.81664844	0.39084543

4 Discussion

4.1 Respiration measurements

To my knowledge, no further study reports values for the critical oxygen saturation (P_{crit}) and aerobic scope (AS) of *Boreogadus saida*. Thus, these findings have a special significance in weighing the viability of Polar cod under future climatic conditions and indicate how this could possibly affect the entire Arctic ecosystem.

Fish species that are able to regulate their metabolic rate under low oxygen saturation are known as oxygen regulators and understood to be hypoxia tolerant (Ultsch, Jackson et al. 1981, Farrell and Richards 2009, Richards 2009). This study showed that Polar cod regulates its RMR under progressive hypoxia (Figure 10). Due to the additional energy demand caused by the swimming activity during the swim tunnel experiments, the MMR could not be kept constant over the entire oxygen range compared to the RMR. Initially, MMR was maintained at a constant level, with metabolic up-regulation at 45 % PO_2 , followed by down-regulation, which can also be observed in oxygen conformers (Figure 11). The energy consumed to swim against the artificially generated and steadily increasing water flow, in addition to oxygen regulation mechanisms, seemed too high to keep the MMR at a constant level in hypoxic waters. Therefore, Polar cod appears as an oxygen conformer in an oxygen range of 5 % and 45 % but is able to regulate its metabolism at oxygen concentrations above 45 % DO in combination with maximum metabolic activity. Looking at the aerobic scope (Figure 13), this pattern is also striking. For a very long period (~45-100 % PO_2) AS could be kept constant. After that, AS gradually decreased and the reached level could be kept constant again by oxygen regulation within an oxygen range of 20-30 % PO_2 . Finally, this was followed by a gradual decrease which was, kept constant until the critical oxygen range was reached (Figure 13).

Compared to metabolic scope of European sea bass (*Dicentrarchus labrax*), Atlantic cod (*Gadus morhua*), common sole (*Solea solea*) and turbot (*Psetta maxima*) reviewed by Chabot and Claireaux (2008), Polar cod started to down regulate its metabolic scope rather late at 45% PO_2 (Appendix Figure 23). The metabolic rate of Sea bass, Atlantic cod and common sole decreased constantly with decreasing oxygen content. Only turbot had an initial phase with constant metabolic rate, between approximately 85 and 100 % PO_2 (Mallekh and Lagardere 2002, Chabot and Claireaux 2008). The regulatory capacity of Polar cod can therefore be classified as very high in comparison to its larger relatives and potential predators. A regulatory

mechanism helping Polar cod to maintain a stable RMR with decreasing oxygen content could be cutaneous respiration.

Gas exchange through the skin (cutaneous respiration) occurs in many different organisms, as in insects, amphibians, fish and even to a small extent in humans (Fitzgerald 1957, Frame, Strauss et al. 1972, Nonnotte and Kirsch 1978, Ferder and Burggren 1985, Grizzle and Thiyagarajah 1987). The ability of fish to get additional O₂ through cutaneous respiration was already described in the literature. Krogh (1904) showed for the first time that cutaneous respiration exists in fish. The gill-clefts of eels were sealed, but the fish were able to maintain up to 60 % of its total oxygen uptake, even under air exposure (Krogh 1904). Influencing and adapting the diffusion capacity of oxygen is probably the most important aspect in regulating cutaneous oxygen uptake. *Periophthalmus*, an amphibious fish genus, uses its cutaneous surface for respiration as well. They adjust their blood flow to enhance the O₂ transport (Wright and Turko 2016). Another example for a skin-breathing fish is plaice, *Pleuronectes platessa*. The importance of cutaneous respiration in fish was showed exemplary with this species by Steffensen et al (1981). Under normoxia cutaneous O₂-uptake amounted 27% of the total O₂-uptake. With progressive hypoxia (at 25 % oxygen saturation) the percentage rose to 37 % (Steffensen, Lomholt et al. 1981).

Further studies showed that cutaneous respiration also is of great importance in polar habitats. Wells (1986) determined the cutaneous respirations of Antarctic icequab, *Rhigophila dearborni*, at ~35 % of the animals total RMR. Another Antarctic fish species with high cutaneous respiration is Antarctic icefish, for which cutaneous respiration accounted for 40 % of the total oxygen uptake (Hemmingsen and Douglas 1970). These high levels of oxygen uptake through the skin seemed to compensate for other structural adaptations to the low temperature habitat and generally low metabolic activity, such as lack of haemoglobin, low erythrocyte numbers or small gill surface area (Hemmingsen 1960, Jakubowski and Rembiszewski 1974, Wells 1986). All these fish have something in common with Polar cod, they have no scales but skin. In fish, neuroepithelial cells, putative oxygen receptor cells, are not only found in the gill filaments, where they lie between the arterial blood flow and the surrounding water, they have also been found in the skin surface (Dunel-Erb, Bailly et al. 1982, Jonz and Nurse 2006, Coolidge, Ciuhandu et al. 2008). These peripheral O₂ chemoreceptors are responsible for several reactions to hypoxia such as hyperventilation or variation of gill vascular resistance (Jonz and Nurse 2006, Porteus, Pollack et al. 2015). To my knowledge, measurements of cutaneous respiration of Polar cod under exclusion of gill respiration have

never been performed so far. The capacity of cutaneous respiration, determined after Steffensen et al. (1981), could give information about the effectiveness and overall importance of cutaneous respiration in Polar cod and its role in adaptation to hypoxia. Therefore, the O₂ uptake across the gills could be subtracted from the total oxygen uptake which will result in the O₂ uptake performed by cutaneous respiration. The low SMR (0.44 μmol O₂/g·h) (Figure 9) of Polar cod could also assist in oxygen regulation. It is already known that adaptation to a low temperature environment is associated with reduced metabolic demand (Guppy and Withers 1999, Guppy 2004). This overall decreased energy demand is likely supporting this extraordinary hypoxia tolerance of Polar cod.

Previous studies have indicated that a link between hypoxia and hypothermia is not only likely, but even similar energy conservation mechanisms might be used (Hochachka 1986, Wood 1991, Bickler and Buck 2007). However, this connection remains unclear until today and there are certain fish groups that are considerably more oxygen sensitive than polar species. For example, different life strategies play an important role. If fish are restricted in their way of life to exclusively aerobic processes, such as continuous swimming species as tuna or trout, they are also less tolerant to oxygen deficiency (Bushnell, Brill et al. 1990, Gamperl, Todgham et al. 2001). Therefore, Polar cod's rather inactive life strategy supports its hypoxia tolerance, resulting in a low P_{crit}. This inactive life strategy is based on its metabolic adaptation to the Arctic temperatures. It is well known that low temperatures reduce the rate of enzymatic reactions, which leads to a decrease in the metabolic rate (Hochachka and Somero 2002). Examples for other hypoxia tolerant fish are species of the genus *Carassius*. The crucian carp (*Carassius carassius*) is possibly the most anoxia-tolerant vertebrate known. It is able to survive months of complete anoxia at temperatures close to 0 °C and it tolerates up to two days of anoxia at 20 °C (data reviewed by Nilsson and Renshaw (2004)). Another *Carassius* species has to be named speaking of hypoxia tolerance, the common goldfish (*Carassius auratus*). It endures 45 h of anoxia at 5 °C and even 22 h at 20 °C (Lutz and Nilsson 2004, Nilsson and Renshaw 2004, Stecyk, Stensløkken et al. 2004). Various mechanisms have been found that allow these fish to survive under oxygen exclusion (Sollid, De Angelis et al. 2003). As a first and simple reaction they reduce their metabolism. Furthermore, they are able to maintain an ion gradient in their hepatocytes during anoxia, therefore they sustain metabolic functions such as the turnover of lactate into ethanol and CO₂. This prevents the accumulation of lactic acid in the cells during exclusion of oxygen. Ethanol and CO₂ can easily be released into the surrounding water by diffusion through the gills (Hyvärinen, Holopainen et al. 1985, Krumschnabel, Schwarzbaum et al. 2000, Nilsson and Renshaw 2004). Moreover, these species have the innate

capacity to adjust their metabolism towards glycolysis and adapt ATP consumption as a response of ambient oxygen concentrations. Glycolysis is an essential pathway to produce energy even under anaerobic conditions when oxygen levels fall below the thresholds for oxidative phosphorylation. *Carassius* species are able to elevate this anaerobic ATP production and additionally reduce ATP consumption through metabolic depression (reviewed by Nilsson and Renshaw (2004)). To ensure enough glucose to run glycolysis, the crucian carp has large glycogen storage in its muscles and liver (30 % of liver wet mass is glycogen) (Hyvärinen, Holopainen et al. 1985). This keeps the ATP level in balance, prevents brain damage and enables it to survive. It is assumable that *B. saida* uses this metabolic pathway as well.

Besides this anaerobic pathway using glucose, there is another energy source that is available in relatively large quantities in fish: lipids. Lipid oxidation was found to account for an important fraction of the energy demand in fish under exercise (Sidell, Crockett et al. 1995, Weber and Haman 1996). There are several lipid stores in the fish, for example intramuscular reserves, which provide lipids that can be oxidized in the locomotor muscles when energy is needed. The breakdown of fatty acids occurs gradually in four individual reactions in the mitochondrial matrix. The end product is acetyl-CoA molecules which can then be oxidized to ATP in the citrate cycle (Sheridan 1988, Weber and Zwingelstein 1995, Weber and Haman 1996). The constantly high oxygen consumption rates of polar cod during the experiments indicate that these aerobic metabolic pathways were used to a greater extent for energy production than glycolysis. Otherwise, a lower oxygen consumption would have been measured. A repetition of these experiments with measurements of ethanol before and after the experiments would give information if, and to what extent, glycolysis is used for ATP production. In order to test this, water samples could be analyzed by high performance liquid chromatography (HPLC). Measuring the lactate and succinate concentrations in the blood of Polar cod, which have been forced to swim under hypoxia, would be another method to prove if this species is able to reduce or even minimize the accumulation of lactic acid when anaerobic metabolic pathways come into play. Provision of ATP by fatty acid oxidation and potentially additional glycolysis together with oxygen uptake through the skin are very likely to be the main reasons why an oxygen regulation can be observed in Polar cod. Additionally, it would be interesting to prove whether Polar cod continues to regulate its RMR at temperatures nearing the upper thermal tolerance limit to determine if oxygen regulation occurs when another stressor is added. It would therefore be useful to repeat the experiments carried out here with an additional temperature ramp. It would be advisable to adopt the temperature ramp of Leo et al. (2017) and Kunz et al. (2016), (0, 3, 6 and 8 °C) as this would allow a comparison between

already collected findings on hypercapnia tolerance and those on hypoxia tolerance under ocean warming.

The strikingly low P_{crit} of 4.81 % (Figure 14) differs greatly from the critical oxygen values of other Gadidae species found in the literature. In comparison, different values for *Gadus ogac* at 1°C are found ranging from 31.68 % to 41.59 % oxygen saturation (50-60 mmHg (31.68-38.02 % oxygen saturation, 4.04-4.85 mg/L)) (Steffensen, Bushnell et al. 1994, Rogers, Urbina et al. 2016). For another relative of *B. saida*, *Gadus morhua*, higher critical oxygen levels were found, as well. Dependent on temperature, P_{crit} ranged from 28.52 % (15 °C) to 15.45 % (10 °C) in juveniles (database Rogers et al. 2016). If one classifies the P_{crit} of the Polar cod in connection with other marine fish species, it can be seen that this value is the lowest of all species presented in the review by Rogers et al (2016) (Appendix Figure 20). In a direct comparison between *B. saida* and its predator in the Svalbard fjord system *Gadus morhua*, it is striking that the P_{crit} of Atlantic cod (16.5 % at 5 °C) is much higher than the P_{crit} of its prey, Polar cod (4.81 % at 2 °C) (Schurmann and Steffensen 1997, Wienerroither, Johannesen et al. 2011, Renaud, Berge et al. 2012). The overall increasing predation pressure exerted on Polar cod by the larger fish species, such as cod and haddock, could be compensated in the future by the different P_{crit} values (Gjertz, Lydersen et al. 2001, Olsen, Aanes et al. 2009, Bjørge, Desportes et al. 2010). A formation of oxygen depleted zones in the Svalbard fjord systems, caused by the above-mentioned environmental changes such as loss of sea ice and increased stratification (Nilsen, Cottier et al. 2008, Szczuciński, Zajączkowski et al. 2009, Promińska, Falck et al. 2018), could also drive the now immigrating species out of the fjords in the future. Therefore, Polar cod could have an advantage over its predators and its low P_{crit} could be understood as a defence strategy against the increasing predation pressure in oxygen-rich waters and an adaptation to future environmental conditions in its main habitat. It has been shown that Polar cod have the ability to remain in Billefjorden, even if the oxygen concentration decreases in the future. Nonetheless, long-time exposure to hypoxia may also cause permanent damage to the organism. Petersen and Gamperl (2010) for example proved this for Atlantic cod, *Gadus morhua*. Long-term exposure to moderate hypoxia (40-45 % PO_2) for six weeks at 10 °C led to decreasing cardiac stroke volume.

In addition to its hypoxia tolerance, rising temperatures up to 8 °C have been set as the long-term upper thermal tolerance limit for Polar cod (Kunz, Frickenhaus et al. 2016). This indicates that the predicted summer air temperature increase for 2050 of maximum 8 °C and 12 °C in 2100 (Førland, Benestad et al. 2011) in connection with oxygen depletion in polar waters

(Promińska, Falck et al. 2018) may not yet pose a threat to the Polar cod. This tolerance to environmental change makes this key Arctic species even more valuable to the Arctic food web.

4.2 Swimming performance

Arctic fishes have to adapt to temperatures close to or even below 0 °C. In parallel, the energetic costs of swimming are as high as for fishes living in temperate regions (Scholander, Flagg et al. 1953). In combination with the higher water viscosity due to the low water temperatures, swimming in the cold is more energy intensive. This can be seen in notothenoids, for which, based on their oxygen consumption, swimming is twice as energy demanding as for temperate species (Wohlschlag 1960). As an adaptation to higher energy demands, muscle ATPase, cytochrome C oxidase and citrate synthase activities are increased in polar species (Johnston and Goldspink 1975, Crockett and Sidell 1990). In addition, the mitochondrial content of polar species is also higher than that of temperate species. Experiments showed that the muscular mitochondria density of some Antarctic species was 60 % higher than in fish from temperate zones (Johnston, Camm et al. 1988). Despite all these adaptations to the environmental conditions in the polar regions, aerobic swimming performance is still limited by the availability of oxygen. The research around the critical swimming speed under hypoxia is numerous (Bushnell, Steffensen et al. 1984, Herbert and Steffensen 2005, Fitzgibbon, Strawbridge et al. 2007, Domenici, Herbert et al. 2013, Claireaux and Chabot 2016, Kunz, Claireaux et al. 2018), but so far, the knowledge about the influence of hypoxia on the swimming performance of Polar cod is limited.

In general, existing studies identified reduced swimming performance as a direct effect of hypoxia (Jourdan-Pineau, Dupont-Prinet et al. 2009, Petersen and Gamperl 2010, Fu, Brauner et al. 2011). In this study, Polar cod also showed a significant decrease of total swimming time ($p = 0.017$), burst counts ($p = 0.025$) and U_{crit} ($p = 0.044$) with progressing hypoxia (Table 5, Table 4, Figure 17). Increasing resting periods and generally reduced swimming time as a response to hypoxia (Table 5, Table 10) have also been found for other species including *Gadus morhua*, *Cyprinus carpio* and *Cynoscion regalis* (Nilsson, Rosen et al. 1993, Nilsson and Renshaw 2004, Herbert and Steffensen 2005, Brady, Targett et al. 2009). The reduction of swimming (speed) is a mechanism to decrease the energy demand and helps the fish to remain metabolic action in its available aerobic scope, reducing the stress level to a minimum (Claireaux and Chabot 2005, Chapman and McKenzie 2009).

U_{crit} and MMR seem to be species-specific, have a high variability and stand for a diverse performance potential (metabolic range) (Fitzgibbon, Strawbridge et al. 2007). Therefore, interspecific comparisons are relatively difficult, since differences in the measuring method and the U_{crit} protocol can also lead to considerable differences (Bushnell, Steffensen et al. 1984).

Furthermore, intraspecific comparisons should also be made with caution as the body length and mass have a significant influence on the MMR and therefore affect the individual U_{crit} (Gallaugh, Thorarensen et al. 2001, Rodnick, Gamperl et al. 2004). Nevertheless, the constantly high U_{crit} under progressive hypoxia supports the theory that Polar cod had partially resorted to anaerobic metabolism and aerobic fatty acid oxidation to support swimming performance at higher velocities (Figure 17). The simultaneous absence of burst appearance beginning at 25 % PO_2 reinforces the assumption that the contribution of anaerobic metabolism to energy production in *B. saida* must be low, since anaerobically fuelled white muscles are used for kick-and-glide swimming (bursts) (Batty and Wardle 1979, Videler 1981). Kunz et al. (2018) already noted that Polar cod showed very little or no bursts under different temperature treatments combined with hypercapnia. The authors furthermore determined an anaerobically fuelled swimming capacity of Polar cod of 0 – 5.7 %. Additionally, the up-regulation of MMR at ~45 % PO_2 (Figure 11) can also be regarded as evidence of aerobic metabolic activity, while down-regulation would rather have supported the occurrence of anaerobic activity. In other polar species, including fish in the Antarctic, a low potential for anaerobic glycolysis has already been shown (Dunn and Johnston 1986, Davison, Forster et al. 1988).

Moreover, the average burst counts per minute 12.61 ± 9.39 (Table 4) under normoxia were much lower compared to findings of Kunz et al. (2018) with burst counts of 11.40 ± 3.40 within 30 sec (measured at ~0 °C and normocapnia), and extremely low compared to other temperate species, e.g. European sea bass, *Dicentrarchus labrax*, bursted 84 times in 30 seconds at U_{crit} velocities and 23 °C (Marras, Claireaux et al. 2010). This low capacity of anaerobic swimming could be a big disadvantage for the already very inert species, since kick-and-glide swimming is an essential escape reaction in response to predator encounters (Beamish 1978). One of the immigrating fish species to Svalbard fjord system feeding on Polar cod is Atlantic cod (Simpson, Jennings et al. 2011, Renaud, Berge et al. 2012). With 15.45 % (at 10 °C) (Rogers, Urbina et al. 2016) its P_{crit} is clearly below Polar cod's threshold of anaerobic swimming. Therefore, the predation pressure on Polar cod would increase as its ability to escape predators decreases under hypoxia.

Comparing hypercapnia (1170 μ atm CO_2) together with temperatures above 0 °C (3, 6, 8 °C), *B. saida* also revealed an increase in MMR, but a simultaneous decrease in maximum swimming velocities (Kunz, Claireaux et al. 2018). In the present study, a significant decrease could only be observed between treatments with 100 % and 10 % PO_2 ($p = 0.031$) (Table 6). Kunz et al. (2018) suggested that elevated metabolic activity under hypercapnia was due to

other mechanisms than swimming activity. They hypothesized that the gills are likely involved in elevated energy demands. Modifications of the gill structure, such as an increase in gill soft tissue, and blood oxygen carrying capacity are essential to perform under hypoxia (Bushnell, Steffensen et al. 1984, Petersen and Gamperl 2010, Fu, Brauner et al. 2011). Such an increase of gill tissue led to an increase of 5 - 7 % of the whole-animal oxygen consumption under 2200 $\mu\text{atm CO}_2$ of *Gadus morhua* (Kreiss, Michael et al. 2015). In the present study, signs for increased gill activity can be found in the increased oxygen consumption for both RMR and MMR under moderate hypoxia (with climax at ~35 % (RMR) and ~45 % PO_2 (MMR)) (Figure 12). After the climax, RMR remained at a constant level, whereas MMR began to steadily decline afterwards. However, no clear shift to white muscle activity was observed, swimming at maximum water velocities could not be sustained by aerobic metabolism alone and it would be important to know the involvement of the anaerobic metabolic pathways. Thus, the build-up of an oxygen debt following exhaustive exercise should be investigated by additional measurement of post-exercise oxygen consumption (EPOC) and could reflect the costs of recovering homeostasis and replenishing substrates in the white muscle (Wood 1991, Richards, Heigenhauser et al. 2002).

5 Conclusion

In conclusion, the present study revealed that Polar cod is an extremely hypoxia tolerant fish species, which was able to handle oxygen saturations down to a P_{crit} of 4.81 % PO_2 . However, hypoxia had a strong impact on MMR and swimming performance parameters of *B. saida*. Although progressive hypoxia did not significantly impact U_{gait} , the total number of bursts and total active swimming time decreased significantly. These findings indicate that rather other swimming performance parameters, such as actual swimming duration and capacity of anaerobic swimming, than critical water velocities (U_{crit}) will challenge Polar cod under future environmental conditions. Especially the loss of anaerobic swimming capacity due to hypoxia may endanger this species in regard to predator-prey-interactions and loss of escape reactions. Another striking aspect of the reaction of Polar cod to hypoxia was found during this study: the species was able to maintain an almost constant RMR though oxygen regulation over an oxygen range from 5 to 100 % oxygen saturation. Furthermore, neither RMR nor MMR decreased below the SMR level of $0.44 \mu\text{mol O}_2/\text{g}\cdot\text{h}$, whereas MMR was initially regulated until 45 % PO_2 followed by a decrease with decreasing oxygen saturations.

Translating the present results onto the population level, escape response of Polar cod during predator interactions could be negatively affected under future water conditions. However, this species may still has an advantage though its hypoxia tolerance over immigrating species with a higher P_{crit} . On the other hand, this study could not conclusively identify which potential long-term damage hypoxia could cause for the organism. The low P_{crit} together with its long-term upper thermal tolerance limit of 8°C (Kunz, Frickenhaus et al. 2016), equip Polar cod very well for the temperatures predicted for Svalbard in the near future (Førland, Benestad et al. 2011). Therefore, it is very likely that Polar cod will keep its valuable role in the Arctic food web under climate change.

6 References

- Baktoft, H., et al. (2016). "Phenotypic variation in metabolism and morphology correlating with animal swimming activity in the wild: relevance for the OCLTT (oxygen-and capacity-limitation of thermal tolerance), allocation and performance models." Conservation physiology **4**(1): cov055.
- Batty, R. and C. Wardle (1979). "Restoration of glycogen from lactic acid in the anaerobic swimming muscle of plaice, *Pleuronectes platessa* L." Journal of Fish Biology **15**(5): 509-519.
- Beamish, F. W. (1978). "Swimming capacity." Fish physiology **7**: 101-187.
- Bickler, P. E. and L. T. Buck (2007). "Hypoxia tolerance in reptiles, amphibians, and fishes: life with variable oxygen availability." Annu. Rev. Physiol. **69**: 145-170.
- Bjørge, A., et al. (2010). "Introduction: the harbour seal (*Phoca vitulina*)-a global perspective." NAMMCO Scientific Publications **8**: 7-11.
- Bradstreet, M. S. (1982). "Occurrence, habitat use, and behavior of seabirds, marine mammals, and Arctic cod at the Pond Inlet ice edge." Arctic: 28-40.
- Brady, D. C., et al. (2009). "Behavioral responses of juvenile weakfish (*Cynoscion regalis*) to diel-cycling hypoxia: swimming speed, angular correlation, expected displacement, and effects of hypoxia acclimation." Canadian Journal of Fisheries and Aquatic Sciences **66**(3): 415-424.
- Brett, J. (1964). "The respiratory metabolism and swimming performance of young sockeye salmon." Journal of the Fisheries Board of Canada **21**(5): 1183-1226.
- Bushnell, P., et al. (1984). "Oxygen consumption and swimming performance in hypoxia-acclimated rainbow trout *Salmo gairdneri*." Journal of Experimental Biology **113**(1): 225-235.
- Bushnell, P. G., et al. (1990). "Cardiorespiratory responses of skipjack tuna (*Katsuwonus pelamis*), yellowfin tuna (*Thunnus albacares*), and bigeye tuna (*Thunnus obesus*) to acute reductions of ambient oxygen." Canadian Journal of Zoology **68**(9): 1857-1865.
- Bushnell, P. G., et al. (1984). "Oxygen consumption and swimming performance in hypoxia-acclimated rainbow trout *Salmo gairdneri*." Journal of Experimental Biology **113**(1): 225-235.
- Caldeira, K. and M. E. Wickett (2005). "Ocean model predictions of chemistry changes from carbon dioxide emissions to the atmosphere and ocean." Journal of Geophysical Research: Oceans **110**(C9).
- Chabot, D. and G. Claireaux (2008). "Environmental hypoxia as a metabolic constraint on fish: the case of Atlantic cod, *Gadus morhua*." Marine Pollution Bulletin **57**(6-12): 287-294.
- Chabot, D., et al. (2016). "The determination of standard metabolic rate in fishes." J Fish Biol **88**(1): 81-121.

- Chapman, L. J. and D. J. McKenzie (2009). Behavioral responses and ecological consequences. Fish physiology, Elsevier. **27**: 25-77.
- Claireaux, G. and D. Chabot (2005). A review of the impact of environmental hypoxia on fish: the case of Atlantic cod. Comparative Biochemistry and Physiology - Part A: Molecular & Integrative Physiology, Elsevier Science Inc 230 Park Ave, New York, NY 10169 USA.
- Claireaux, G. and D. Chabot (2016). "Responses by fishes to environmental hypoxia: integration through Fry's concept of aerobic metabolic scope." Journal of Fish Biology **88**(1): 232-251.
- Claireaux, G. and C. Lefrançois (2007). "Linking environmental variability and fish performance: integration through the concept of scope for activity." Philosophical Transactions of the Royal Society of London B: Biological Sciences **362**(1487): 2031-2041.
- Clark, T. D., et al. (2013). "Aerobic scope measurements of fishes in an era of climate change: respirometry, relevance and recommendations." Journal of Experimental Biology **216**(15): 2771-2782.
- Cohen, D. M., et al. (1990). "Gadiform fishes of the world." FAO fisheries synopsis **10**(125).
- Collins, M., et al. (2013). Long-term climate change: projections, commitments and irreversibility. Climate Change 2013-The Physical Science Basis: Contribution of Working Group I to the Fifth Assessment Report of the Intergovernmental Panel on Climate Change, Cambridge University Press: 1029-1136.
- Coolidge, E. H., et al. (2008). "A comparative analysis of putative oxygen-sensing cells in the fish gill." Journal of Experimental Biology **211**(8): 1231-1242.
- Craig, P., et al. (1982). "Ecological studies of Arctic cod (*Boreogadus saida*) in Beaufort Sea coastal waters, Alaska." Canadian Journal of Fisheries and Aquatic Sciences **39**(3): 395-406.
- Crawford, R. and J. Jorgenson (1996). "Quantitative studies of Arctic cod (*Boreogadus saida*) schools: important energy stores in the Arctic food web." Arctic: 181-193.
- Crawford, R., et al. (2012). "Water mass and bathymetric characteristics of polar cod habitat along the continental shelf and slope of the Beaufort and Chukchi seas." Polar Biology **35**(2): 179-190.
- Crockett, E. L. and B. D. Sidell (1990). "Some pathways of energy metabolism are cold adapted in Antarctic fishes." Physiological Zoology **63**(3): 472-488.
- Davison, W., et al. (1988). "Recovery from exhausting exercise in an Antarctic fish, *Pagothenia borchgrevinki*." Polar Biology **8**(3): 167-171.
- Diaz, R. J. and R. Rosenberg (1995). "Marine benthic hypoxia: a review of its ecological effects and the behavioural responses of benthic macrofauna." Oceanography and marine biology. An annual review **33**: 245-203.

- Domenici, P., et al. (2013). The effect of hypoxia on fish swimming performance and behaviour. Swimming physiology of fish, Springer, Berlin, Heidelberg,: 129-159.
- Domenici, P., et al. (2000). "The effect of progressive hypoxia on swimming activity and schooling in Atlantic herring." Journal of Fish Biology **57**(6): 1526-1538.
- Drost, H. E., et al. (2014). "Upper thermal limits of cardiac function for Arctic cod *Boreogadus saida*, a key food web fish species in the Arctic Ocean." J Fish Biol **84**(6): 1781-1792.
- Dunel-Erb, S., et al. (1982). "Neuroepithelial cells in fish gill primary lamellae." Journal of Applied Physiology **53**(6): 1342-1353.
- Dunn, J. F. and I. A. Johnston (1986). "Metabolic constraints on burst-swimming in the Antarctic teleost *Notothenia neglecta*." Marine Biology **91**(4): 433-440.
- Eriksen, E., et al. (2015). "The effect of recent warming on polar cod and beaked redfish juveniles in the Barents Sea." Regional Studies in Marine Science **2**: 105-112.
- Eriksen, E., et al. (2015). "The effect of recent warming on polar cod and beaked redfish juveniles in the Barents Sea." Regional Studies in Marine Science **2**: 105-112.
- Farrell, A. P. and J. G. Richards (2009). Defining hypoxia: an integrative synthesis of the responses of fish to hypoxia. Fish physiology, Academic Press. **27**: 487-503.
- Ferder, M. E. and W. W. Burggren (1985). "Cutaneous gas exchange in vertebrates: design, patterns, control and implications." Biological Reviews **60**(1): 1-45.
- Fitzgerald, L. R. (1957). "Cutaneous respiration in man." Physiological reviews **37**(3): 325-336.
- Fitzgibbon, Q., et al. (2007). "Metabolic scope, swimming performance and the effects of hypoxia in the mullock, *Argyrosomus japonicus* (Pisces: Sciaenidae)." Aquaculture **270**(1-4): 358-368.
- Fitzgibbon, Q. P., et al. (2007). "Metabolic scope, swimming performance and the effects of hypoxia in the mullock, *Argyrosomus japonicus* (Pisces: Sciaenidae)." Aquaculture **270**(1-4): 358-368.
- Førland, E. J., et al. (2011). "Temperature and precipitation development at Svalbard 1900–2100." Advances in Meteorology **2011**.
- Førland, E. J., et al. (2009). Climate development in North Norway and the Svalbard region during 1900–2100.
- Fossheim, M., et al. (2015). "Recent warming leads to a rapid borealization of fish communities in the Arctic." Nature Climate Change **5**(7): 673.
- Frame, G. W., et al. (1972). "Carbon dioxide emission of the human arm and hand." Journal of Investigative Dermatology **59**(2): 155-158.

- Fu, S.-J., et al. (2011). "The effect of acclimation to hypoxia and sustained exercise on subsequent hypoxia tolerance and swimming performance in goldfish (*Carassius auratus*)."
Journal of Experimental Biology **214**(12): 2080-2088.
- Gallaugh, P. E., et al. (2001). "Effects of high intensity exercise training on cardiovascular function, oxygen uptake, internal oxygen transport and osmotic balance in chinook salmon (*Oncorhynchus tshawytscha*) during critical speed swimming." Journal of Experimental Biology **204**(16): 2861-2872.
- Gamperl, A. K., et al. (2001). "Recovery of trout myocardial function following anoxia: preconditioning in a non-mammalian model." American Journal of Physiology-Regulatory, Integrative and Comparative Physiology **281**(6): R1755-R1763.
- Gjertz, I., et al. (2001). "Distribution and diving of harbour seals (*Phoca vitulina*) in Svalbard." Polar Biology **24**(3): 209-214.
- Grizzle, J. M. and A. Thiyagarajah (1987). "Skin histology of *Rivulus ocellatus marmoratus*: apparent adaptation for aerial respiration." Copeia **1987**(1): 237-240.
- Guppy, M. (2004). "The biochemistry of metabolic depression: a history of perceptions." Comparative Biochemistry and Physiology Part B: Biochemistry and Molecular Biology **139**(3): 435-442.
- Guppy, M. and P. Withers (1999). "Metabolic depression in animals: physiological perspectives and biochemical generalizations." Biological Reviews **74**(1): 1-40.
- Hemmingsen, A. M. (1960). "Energy metabolism as related to body size and respiratory surface, and its evolution." Reports of the Steno Memorial Hospital (Copenhagen) **13**: 1-110.
- Hemmingsen, E. A. and E. L. Douglas (1970). "Respiratory characteristics of the hemoglobin-free fish *Chaenocephalus aceratus*." Comparative biochemistry and physiology **33**(4): 733-744.
- Herbert, N. and J. Steffensen (2005). "The response of Atlantic cod, *Gadus morhua*, to progressive hypoxia: fish swimming speed and physiological stress." Marine Biology **147**(6): 1403-1412.
- Herbert, N. A. and J. F. Steffensen (2005). "The response of Atlantic cod, *Gadus morhua*, to progressive hypoxia: fish swimming speed and physiological stress." Marine Biology **147**(6): 1403-1412.
- Hochachka, P. W. (1986). "Defense strategies against hypoxia and hypothermia." Science **231**(4735): 234-241.
- Hochachka, P. W. and G. N. Somero (2002). Biochemical adaptation: mechanism and process in physiological evolution, Oxford University Press.
- Hoegh-Guldberg, O. and J. F. Bruno (2010). "The impact of climate change on the world's marine ecosystems." Science **328**(5985): 1523-1528.

- Hognestad, P. T. (1966). Observations on polar cod in the Barents Sea, ICES Journal of Marine Science.
- Hognestad, P. T. (1968). Polar cod, *Boreogadus saida* Lep, in Norwegian waters, Universitetsforlaget.
- Hop, H. and H. Gjørseter (2013). "Polar cod (*Boreogadus saida*) and capelin (*Mallotus villosus*) as key species in marine food webs of the Arctic and the Barents Sea." Marine Biology Research **9**(9): 878-894.
- Hop, H., et al. (1997). Population structure and feeding ecology of Arctic cod schools in the Canadian High Arctic. Fish ecology in Arctic North America. American fisheries society symposium.
- Hyvärinen, H., et al. (1985). "Anaerobic wintering of crucian carp (*Carassius carassius* L.)-I. Annual dynamics of glycogen reserves in nature." Comparative Biochemistry and Physiology Part A: Physiology **82**(4): 797-803.
- Hyvärinen, H., et al. (1985). "Anaerobic wintering of crucian carp (*Carassius carassius* L.)-I. Annual dynamics of glycogen reserves in nature." Comparative Biochemistry and Physiology Part A: Physiology **82**(4): 797-803.
- IPCC (2007). "IPCC fourth assessment report: climate change 2007." Intergovernmental Panel on Climate Change **4**: 213-252.
- Jakubowski, M. and J. Rembiszewski (1974). "Vascularization and size of respiratory surfaces of gills and skin in the Antartic fish *Gymnodraco acuticeps* Boul.(Bathydraconidae)." Bulletin of the Polish Academy of Sciences: Biological Sciences **22**(5): 305-313.
- Johnston, I. A., et al. (1988). "Specialisations of swimming muscles in the pelagic Antarctic fish *Pleuragramma antarcticum*." Marine Biology **100**(1): 3-12.
- Johnston, I. A. and G. Goldspink (1975). "Thermodynamic activation parameters of fish myofibrillar ATPase enzyme and evolutionary adaptations to temperature." Nature **257**(5527): 620.
- Jonz, M. G. and C. A. Nurse (2006). "Ontogenesis of oxygen chemoreception in aquatic vertebrates." Respiratory physiology & neurobiology **154**(1-2): 139-152.
- Jourdan-Pineau, H., et al. (2009). "An investigation of metabolic prioritization in the European sea bass, *Dicentrarchus labrax*." Physiological and Biochemical Zoology **83**(1): 68-77.
- Keeling, R. F., et al. (2009). "Ocean deoxygenation in a warming world."
- Kjesbu, O. S., et al. (2014). "Synergies between climate and management for Atlantic cod fisheries at high latitudes." Proceedings of the National Academy of Sciences **111**(9): 3478-3483.
- Kreiss, C. M., et al. (2015). "Ocean warming and acidification modulate energy budget and gill ion regulatory mechanisms in Atlantic cod (*Gadus morhua*)." Journal of Comparative Physiology B **185**(7): 767-781.

- Krogh, A. (1904). "Some experiments on the cutaneous respiration of vertebrate animals 1, 2." Skandinavisches Archiv für Physiologie **16**(2): 348-357.
- Krogh, A. (1914). The quantitative relation between temperature and standard metabolism in animals.
- Krumschnabel, G., et al. (2000). "Oxygen-dependent energetics of anoxia-tolerant and anoxia-intolerant hepatocytes." Journal of Experimental Biology **203**(5): 951-959.
- Kunz, K. L., et al. (2018). "Aerobic capacities and swimming performance of polar cod (*Boreogadus saida*) under ocean acidification and warming conditions." Journal of Experimental Biology **221**(21): jeb184473.
- Kunz, K. L., et al. (2016). "New encounters in Arctic waters: a comparison of metabolism and performance of polar cod (*Boreogadus saida*) and Atlantic cod (*Gadus morhua*) under ocean acidification and warming." Polar Biology **39**(6): 1137-1153.
- Kwok, R. and N. Untersteiner (2011). "The thinning of Arctic sea ice." Phys. Today **64**(4): 36-41.
- Leo, E., et al. (2017). "Mitochondrial acclimation potential to ocean acidification and warming of Polar cod (*Boreogadus saida*) and Atlantic cod (*Gadus morhua*)." Front Zool **14**: 21.
- Lønne, O. and B. Gulliksen (1989). "Size, age and diet of polar cod, *Boreogadus saida* (Lepechin 1773), in ice covered waters." Polar Biology **9**(3): 187-191.
- Lutz, P. L. and G. E. Nilsson (2004). "Vertebrate brains at the pilot light." Respiratory physiology & neurobiology **141**(3): 285-296.
- Majewski, A. R., et al. (2016). "Distribution and diet of demersal Arctic Cod, *Boreogadus saida*, in relation to habitat characteristics in the Canadian Beaufort Sea." Polar Biology **39**(6): 1087-1098.
- Mallekh, R. and J. Lagardere (2002). "Effect of temperature and dissolved oxygen concentration on the metabolic rate of the turbot and the relationship between metabolic scope and feeding demand." Journal of Fish Biology **60**(5): 1105-1115.
- Mark, F. C. and A. Wisotzki (2018). Physical oceanography during HEINCKE cruise HE519, PANGAEA.
- Marras, S., et al. (2010). "Individual variation and repeatability in aerobic and anaerobic swimming performance of European sea bass, *Dicentrarchus labrax*." Journal of Experimental Biology **213**(1): 26-32.
- Matear, R. and A. Hirst (2003). "Long-term changes in dissolved oxygen concentrations in the ocean caused by protracted global warming." Global Biogeochemical Cycles **17**(4).
- Meinshausen, M., et al. (2011). "The RCP greenhouse gas concentrations and their extensions from 1765 to 2300." Climatic change **109**(1-2): 213.

Neill, W. H. and J. D. Bryan (1991). "Responses of fish to temperature and oxygen, and response integration through metabolic scope." Aquaculture and water quality **3**: 30-57.

Neill, W. H., et al. (1994). "Ecophysiology of marine fish recruitment: a conceptual framework for understanding interannual variability." Netherlands Journal of Sea Research **32**(2): 135-152.

Nilsen, F., et al. (2008). "Fjord–shelf exchanges controlled by ice and brine production: the interannual variation of Atlantic Water in Isfjorden, Svalbard." Continental Shelf Research **28**(14): 1838-1853.

Nilsson, G. E. and G. M. Renshaw (2004). "Hypoxic survival strategies in two fishes: extreme anoxia tolerance in the North European crucian carp and natural hypoxic preconditioning in a coral-reef shark." Journal of Experimental Biology **207**(18): 3131-3139.

Nilsson, G. E., et al. (1993). "Anoxic depression of spontaneous locomotor activity in crucian carp quantified by a computerized imaging technique." Journal of Experimental Biology **180**(1): 153-162.

Nonnotte, G. and R. Kirsch (1978). "Cutaneous respiration in seven sea-water teleosts." Respiration physiology **35**(2): 111-118.

Olsen, E., et al. (2009). "Cod, haddock, saithe, herring, and capelin in the Barents Sea and adjacent waters: a review of the biological value of the area." ICES Journal of Marine Science **67**(1): 87-101.

Orlova, E. L., et al. (2009). "Trophic relations of capelin *Mallotus villosus* and polar cod *Boreogadus saida* in the Barents Sea as a factor of impact on the ecosystem." Deep Sea Research Part II: Topical Studies in Oceanography **56**(21-22): 2054-2067.

Overland, J. E. and M. Wang (2013). "When will the summer Arctic be nearly sea ice free?" Geophysical Research Letters **40**(10): 2097-2101.

Petersen, L. and A. Gamperl (2010). "Effect of acute and chronic hypoxia on the swimming performance, metabolic capacity and cardiac function of Atlantic cod (*Gadus morhua*)." Journal of Experimental Biology **213**(5): 808-819.

Polyakov, I. V., et al. (2010). "Arctic Ocean warming contributes to reduced polar ice cap." Journal of Physical Oceanography **40**(12): 2743-2756.

Ponomarenko, V. (1968). "Some data on the distribution and migrations of polar cod in the seas of the Soviet Arctic." Rapp PV Reun Cons Perm Int Explor Mer **158**: 131-135.

Porteus, C. S., et al. (2015). "A role for nitric oxide in the control of breathing in zebrafish (*Danio rerio*)." Journal of Experimental Biology **218**(23): 3746-3753.

Pörtner, H. O. (2010). "Oxygen-and capacity-limitation of thermal tolerance: a matrix for integrating climate-related stressor effects in marine ecosystems." Journal of Experimental Biology **213**(6): 881-893.

Pörtner, H. O., et al. (2017). "Oxygen-and capacity-limited thermal tolerance: bridging ecology and physiology." Journal of Experimental Biology **220**(15): 2685-2696.

Pörtner, H. O., et al. (2014). Ocean systems. Climate change 2014: impacts, adaptation, and vulnerability. Part A: global and sectoral aspects. contribution of working group II to the fifth assessment report of the intergovernmental panel on climate change, Cambridge University Press: 411-484.

Pörtner, H. O. and R. Knust (2007). "Climate change affects marine fishes through the oxygen limitation of thermal tolerance." Science **315**(5808): 95-97.

Pörtner, H. O. and G. Lannig (2009). Oxygen and capacity limited thermal tolerance. Fish physiology, Academic Press. **27**: 143-191.

Promińska, A., et al. (2018). "Interannual variability in hydrography and water mass distribution in Hornsund, an Arctic fjord in Svalbard." Polar Research **37**(1): 1495546.

Renaud, P. E., et al. (2012). "Is the poleward expansion by Atlantic cod and haddock threatening native polar cod, *Boreogadus saida*?" Polar Biology **35**(3): 401-412.

Richards, J. G. (2009). Metabolic and molecular responses of fish to hypoxia. Fish physiology, Academic Press. **27**: 443-485.

Richards, J. G., et al. (2002). "Lipid oxidation fuels recovery from exhaustive exercise in white muscle of rainbow trout." American Journal of Physiology-Regulatory, Integrative and Comparative Physiology **282**(1): R89-R99.

Rodnick, K., et al. (2004). "Thermal tolerance and metabolic physiology among redband trout populations in south-eastern Oregon." Journal of Fish Biology **64**(2): 310-335.

Rogers, N. J., et al. (2016). "A new analysis of hypoxia tolerance in fishes using a database of critical oxygen level (P_{crit})." Conservation physiology **4**(1).

Scholander, P., et al. (1953). "Climatic adaptation in arctic and tropical poikilotherms." Physiological Zoology **26**(1): 67-92.

Schurmann, H. and J. S. Christiansen (1994). "Behavioral thermoregulation and swimming activity of two Arctic teleosts (subfamily *Gadinae*)—the polar cod (*Boreogadus saida*) and the navaga (*Eleginus navaga*)." Journal of thermal biology **19**(3): 207-212.

Schurmann, H. and J. Steffensen (1997). "Effects of temperature, hypoxia and activity on the metabolism of juvenile Atlantic cod." Journal of Fish Biology **50**(6): 1166-1180.

Scott, W. and M. Scott (1988). Atlantic fishes of Canada Canadian Bulletin of Fisheries and Aquatic Science, 219, University of Toronto Press, Toronto, Canada.

Sheridan, M. A. (1988). "Lipid dynamics in fish: aspects of absorption, transportation, deposition and mobilization." Comparative Biochemistry and Physiology Part B: Comparative Biochemistry **90**(4): 679-690.

Sidell, B. D., et al. (1995). "Antarctic fish tissues preferentially catabolize monoenoic fatty acids." Journal of Experimental Zoology **271**(2): 73-81.

Simpson, S. D., et al. (2011). "Continental shelf-wide response of a fish assemblage to rapid warming of the sea." Current Biology **21**(18): 1565-1570.

Sollid, J., et al. (2003). "Hypoxia induces adaptive and reversible gross morphological changes in crucian carp gills." Journal of Experimental Biology **206**(20): 3667-3673.

Stecyk, J. A., et al. (2004). "Maintained cardiac pumping in anoxic crucian carp." Science **306**(5693): 77-77.

Steffensen, J., et al. (1994). "Oxygen consumption in four species of teleosts from Greenland: no evidence of metabolic cold adaptation." Polar Biology **14**(1): 49-54.

Steffensen, J. F., et al. (1981). "The relative importance of skin oxygen uptake in the naturally buried plaice, *Pleuronectes platessa*, exposed to graded hypoxia." Respiration physiology **44**(3): 269-275.

Storch, D., et al. (2014). "Climate sensitivity across marine domains of life: limits to evolutionary adaptation shape species interactions." Global change biology **20**(10): 3059-3067.

Szczuciński, W., et al. (2009). "Sediment accumulation rates in subpolar fjords—Impact of post-Little Ice Age glaciers retreat, Billefjorden, Svalbard." Estuarine, Coastal and Shelf Science **85**(3): 345-356.

Ultsch, G. R., et al. (1981). "Metabolic oxygen conformity among lower vertebrates: the toadfish revisited." Journal of comparative physiology **142**(4): 439-443.

Videler, J. (1981). Swimming movements, body structure and propulsion in cod *Gadus morhua*. Symp. Zool. Soc. Lond.

Weber, J.-M. and F. Haman (1996). "Pathways for metabolic fuels and oxygen in high performance fish." Comparative Biochemistry and Physiology Part A: Physiology **113**(1): 33-38.

Weber, J.-M. and G. Zwingelstein (1995). Circulatory substrate fluxes and their regulation. Biochemistry and molecular biology of fishes, Elsevier. **4**: 15-32.

Welch, H. E., et al. (1992). "Energy flow through the marine ecosystem of the Lancaster Sound region, arctic Canada." Arctic: 343-357.

Welch, H. E., et al. (1993). "Occurrence of Arctic cod (*Boreogadus saida*) schools and their vulnerability to predation in the Canadian High Arctic." Arctic: 331-339.

Wells, R. M. (1986). "Cutaneous oxygen uptake in the Antarctic icequab, *Rhigophila dearborni* (Pisces: Zoarcidae)." Polar Biology **5**(3): 175-179.

Wienerroither, R., et al. (2011). "Atlas of the Barents Sea fishes." IMR/PINRO Joint Report Series **1**(2011): 1-272.

Wohlschlag, D. E. (1960). "Metabolism of an Antarctic fish and the phenomenon of cold adaptation." Ecology **41**(2): 287-292.

Wood, C. M. (1991). "Acid-base and ion balance, metabolism, and their interactions, after exhaustive exercise in fish." Journal of Experimental Biology **160**(1): 285-308.

Wood, S. C. (1991). "Interactions between hypoxia and hypothermia." Annual Review of Physiology **53**(1): 71-85.

Wright, P. A. and A. J. Turko (2016). "Amphibious fishes: evolution and phenotypic plasticity." Journal of Experimental Biology **219**(15): 2245-2259.

Appendix

Table 7 **Fish-tagging.** Serial number of the implanted passive glass transponder (PIT), the fish weight [g], total- and standard length [cm], width [cm] (vertical axis, measured at the thickest point) and depth [cm] (horizontal axis, measured at the thickest point).

No.	PIT No.	Weight [g]	Total length [cm]	Standard length [cm]	Width [cm]	Depth [cm]
1	9900000000638 16	35	19.40	17.8	2.8	2.2
2	50	41	20.6	18.9	3	2.7
3	80	38	19.6	17.7	3	2.5
4	31	63	22.5	20.3	3.7	2.6
5	36	34	19.3	17.6	2.9	2.4
6	95	35	19.9	17.8	3.1	2.2
7	75	49	20.4	18.3	3.7	2.5
8	41	38	20.1	17.9	2.9	2
9	37	53	20.5	18.5	3.1	2.4
10	23	36	19.2	16.8	2.4	1.9
11	0 8	61	22.1	20.2	3.6	2.7
12	85	43	20.5	18	3.1	2.3
13	84	36	19.3	16.9	2.9	1.5
14	0 7	35	18.8	16.7	2.6	1.5
15	22	37	19.7	17.6	2.7	1.8
16	38	43	20.1	18.6	2.7	1.7
17	74	44	20.8	18.7	3	2.3
18	44	28	17.7	15.9	2.6	1.5
19	15	44	21.1	18.5	2.6	1.9
20	51	36	18.9	16.9	3	2.2
21	47	34	19.3	17.1	3.3	2
22	72	34	20.3	18.4	2.4	1.3
23	13	36	18.7	16.7	3	2.1
24	57	26	17	15	2.5	1.6
25	90	29	18.5	16.3	2.4	1.5
26	66	32	17.8	16.2	2.9	1.6
27	97	30	18.2	16.6	2.6	1.2
28	17	62	21.8	19.7	3.4	2.4
29	53	45	20.3	17.9	3.1	2
30	96	32	17.7	16.4	2.6	1.9

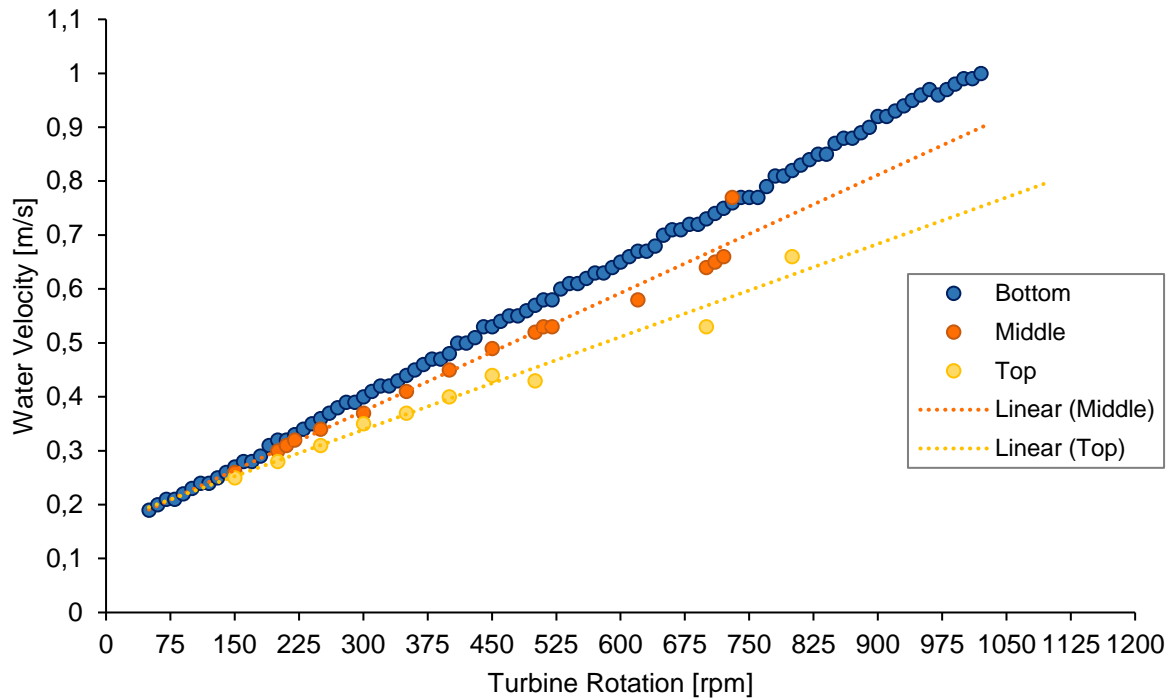


Figure 18 Turbine calibration. The turbine rotation was calibrated using a flowmeter. Turbine rotation was increased in steps of 10 rpm, de corresponding water velocity in m/s were detected with a flowmeter. Water velocity was measured at the bottom of the working section in the swim tunnel. This was repeated randomly for the middle and top layer of the working section. Linear regressions though the values measured in the middle and top region to calculate the corresponding water velocity at 1020 rpm. This calibration data was used to determine the actual water velocity within the swim tunnel.

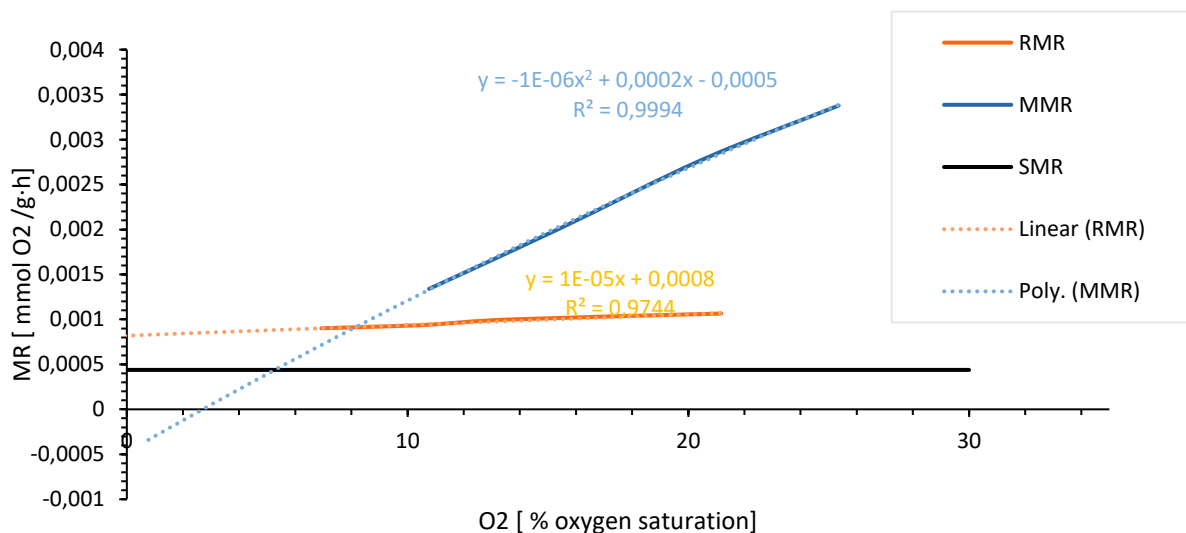


Figure 19 P_{crit} calculation. Shown are SMR (black), RMR (orange), MMR (blue), RMR linear regression line (dotted orange) and MMR polynomial regression line (dotted blue).

Table 8 U_{gait} [rpm and BL/sec] and U_{crit} [rpm and BL/sec] for all fish ordered by the different PO_2 treatments.

Treatment	Fish	U_{gait} [rpm]	U_{gait} [BL/sec]	U_{crit} [rpm]	U_{crit} [BL/sec]
100%	1	394.73	2.20	449.27	2.41
100%	2	360.91	2.39	620.45	3.63
100%	3	421.91	2.79	520.82	3.21
100%	4	346.45	2.03	611.55	3.37
100%	5	327.09	2.05	351.36	2.20
100%	6	573.55	3.49	456.36	2.57
70%	1	484.82	3.49	454.27	2.99
70%	2	531.91	3.49	506.55	3.17
70%	3	363.91	2.54	489.82	3.38
70%	4	512.91	3.49	427.00	2.78
70%	5	265.48	2.05	440.36	3.37
70%	6	334.18	2.03	427.73	2.58
60%	1	324.18	2.04	324.18	2.04
60%	2	502.82	2.75	643.18	3.40
60%	3	480.36	2.57	783.82	3.85
60%	4	308.73	2.54	286.64	2.21
60%	5	402.91	2.40	624.36	3.67
60%	6	350.64	2.03	395.45	2.20
50%	1	243.64	1.70	451.64	2.76
50%	2	555.64	2.99	675.36	3.61
50%	3	447.09	2.20	652.55	3.17
50%	4	316.73	2.03	376.18	2.40
50%	5	377.82	2.36	483.73	2.73
50%	6	486.45	2.75	479.45	2.78
40%	1	472.55	2.92	515.00	3.01
40%	2	382.36	2.36	575.64	3.40
40%	3	358.91	2.05	455.68	2.41
40%	4	NA	NA	335.73	2.25
40%	5	353.09	2.03	373.25	2.05
40%	6	520.18	2.75	485.82	2.51
30%	1	441.36	2.36	455.07	2.36
30%	2	406.55	2.20	537.64	2.78
30%	3	526.82	3.20	662.00	3.86
30%	4	301.64	1.90	541.64	3.17
30%	5	410.45	2.52	452.91	2.69
30%	6	397.27	2.54	309.82	1.90
25%	1	427.36	2.59	370.27	2.20
25%	2	377.27	2.20	569.82	3.19
25%	3	303.36	2.03	589.36	3.41
25%	4	364.00	2.05	607.00	3.37
25%	5	372.55	2.92	517.27	3.10
25%	6	395.91	2.03	542.73	2.57

20%	1	NA	NA	475.45	2.78
20%	2	NA	NA	381.52	2.07
20%	3	300.55	1.87	394.45	2.20
20%	4	360.45	2.20	479.27	2.22
20%	5	544.09	3.38	361.88	2.07
20%	6	NA	NA	756.91	3.56
15%	1	402.45	2.40	456.91	2.59
15%	2	NA	NA	537.91	3.12
15%	3	NA	NA	439.00	2.76
15%	4	NA	NA	541.64	3.17
15%	5	NA	NA	341.58	2.29
15%	6	287.45	1.87	379.09	2.20
10%	1	NA	NA	335.06	2.07
10%	2	NA	NA	287.00	1.85
10%	3	NA	NA	383.73	2.03
10%	4	NA	NA	306.00	1.85
10%	5	NA	NA	329.27	2.17
10%	6	284.09	1.87	305.70	1.90

Table 9 Raw data bursts. Ordered by PO₂ Treatments, TSB = time spent bursting.

Treatment	Fish	Number of bursts	TSB [HH:MM]	TSB with inactive Phases [min]	TSB without in active Phases [min]	Total measurement period [min]	Bursts per min
100%	1	55	14:37-14:47	10	6.17	68.22	8.92
100%	2	616	11:18-11:56	38	36.85	82.13	16.72
100%	3	24	14:27-14:54	27	23.12	38.42	1.04
100%	4	100	11:18-11:35	17	10.27	42.02	9.74
100%	5	16	14:45	1	0.52	38.68	30.97
100%	6	66	11:24-11:38	14	7.98	48.57	8.27
70%	1	66	14:52-15:08	16	6.17	47.08	10.70
70%	2	14	12:01-12:09	8	1.85	49.85	7.57
70%	3	3	15:07-15:15	8	2.55	25.55	1.18
70%	4	26	11:20-11:26	6	3.37	47.88	7.72
70%	5	24	14:41-14:47	6	3.00	32.93	8.00
70%	6	1	12:01-12:04	3	0.45	29.47	2.22
60%	1	1	11:36	1	0.92	13.53	1.09
60%	2	6	15:30-15:38	8	3.17	50.88	1.89
60%	3	92	12:08-12:43	35	11.77	41.22	7.82
60%	4	1	11:45-12:00	15	3.27	20.70	0.31
60%	5	10	11:54-12:04	8	0.63	26.33	15.79
60%	6	3	15:21-15:29	10	0.17	11.53	18.00
50%	1	12	14:51-15:11	20	2.88	13.28	4.16
50%	2	39	11:57	1	0.75	32.02	52.00
50%	3	3	15:28-15:31	3	0.90	3.30	3.33
50%	4	6	11:20-11:32	12	0.63	21.77	9.47
50%	5	156	15:16-15:48	32	16.20	74.33	9.63
50%	6	2	11:36	1	0.73	42.23	2.73

40%	1	24	15:20-15:40	20	15.53	82.42	1.55
40%	2	83	15:05-15:42	37	11.92	65.62	6.97
40%	3	68	11:21-11:29	8	4.83	56.13	14.07
40%	4	0	0	0	0.00	24.83	NA
40%	5	2	11:13-11:19	6	1.00	20.20	2.00
40%	6	83	15:00-15:10	10	3.02	37.75	27.51
30%	1	5	11:48	1	1.00	12.57	5.00
30%	2	43	11:11-11:23	12	4.82	21.27	8.93
30%	3	124	14:48-15:11	23	10.43	69.20	11.88
30%	4	42	11:04-11:07	3	1.72	41.07	24.47
30%	5	54	14:43-15:04	21	7.62	62.32	7.09
30%	6	17	11:10-11:11	1	0.57	41.27	30.00
25%	1	7	14:34	0.25	0.25	13.95	28.00
25%	2	12	12:22-12:24	3	2.28	66.25	5.26
25%	3	42	15:41-16:18	37	15.62	59.95	2.69
25%	4	7	11:37-11:41	4	1.13	22.73	6.18
25%	5	17	15:30-15:38	8	1.13	93.50	15.00
25%	6	4	11:33-11:55	22	1.13	35.93	3.53
20%	1	0	0	0	0.00	44.72	0.00
20%	2	0	0	0	0.00	39.02	0.00
20%	3	49	14:16-14:36	20	6.93	38.00	7.07
20%	4	1	11:07	1	0.82	44.32	1.22
20%	5	115	14:09-14:22	13	10.30	41.13	11.17
20%	6	0	0	0	0.00	30.87	0.00

15%	1	20	11:07-11:18	11	2.22	30.88	9.02
15%	2	0	0	0	0.00	25.80	0.00
15%	3	0	0	0	0.00	9.50	0.00
15%	4	0	0	0	0.00	8.62	0.00
15%	5	0	0	0	0.00	28.17	0.00
15%	6	13	10:50-11:02	12	2.60	37.65	5.00
10%	1	0	0	0	0.00	27.17	0.00
10%	2	0	0	0	0.00	6.60	0.00
10%	3	0	0	0	0.00	3.88	0.00
10%	4	0	0	0	0.00	7.52	0.00
10%	5	0	0	0	0.00	7.15	0.00
10%	6	5	13:40	1	0.73	21.95	6.82

Table 10 Raw data swimming time. Ordered by PO₂ Treatments, TMT = total measurement time, sec. inactive = inactive period per fish in seconds during measurement time.

Treatment	Fish	sec inactive	TMT [HH:MM]	TMT [min]	swimming time [min]	inactive [%]	active [%]
100%	1	527	13:31-14:48	77	68.22	11.41	88.59
100%	2	112	10:21-11:55	84	82.13	2.22	97.78
100%	3	335	14:08-14:52	44	38.42	12.69	87.31
100%	4	1199	10:33-11:35	62	42.02	32.23	67.77
100%	5	919	13:50-14:44	54	38.68	28.36	71.64
100%	6	1106	10:31-11:38	67	48.57	27.51	72.49
70%	1	1315	13:59-15:08	69	47.08	31.76	68.24
70%	2	609	11:08-12:08	60	49.85	16.92	83.08
70%	3	987	14:29-15:11	42	25.55	39.17	60.83
70%	4	607	10:27-11:25	58	47.88	17.44	82.56
70%	5	1624	13:46-14:46	60	32.93	45.11	54.89
70%	6	1052	11:16-12:03	47	29.47	37.30	62.70
60%	1	1288	11:01-11:36	35	13.53	61.33	38.67
60%	2	2467	14:06-15:38	92	50.88	44.69	55.31
60%	3	3767	11:00-12:44	104	41.22	60.37	39.63
60%	4	1878	11:07-11:59	52	20.70	60.19	39.81
60%	5	1660	14:35-15:29	54	26.33	51.23	48.77
60%	6	2668	11:09-12:05	56	11.53	79.40	20.60
50%	1	1843	14:28-15:11	44	13.28	69.81	30.19
50%	2	2759	10:43-12:01	78	32.02	58.95	41.05
50%	3	3462	14:32-15:33	61	3.30	94.59	5.41
50%	4	2114	10:35-11:32	57	21.77	61.81	38.19
50%	5	1540	14:08-15:48	100	74.33	25.67	74.33
50%	6	1786	10:17-11:35	72	42.23	41.34	58.66

40%	1	1655	13:50-15:40	110	82.42	25.08	74.92
40%	2	1583	14:10-15:42	92	65.62	28.68	71.32
40%	3	1252	10:26-11:43	77	56.13	27.10	72.90
40%	4	2470	13:57-15:03	66	24.83	62.37	37.63
40%	5	1728	10:28-11:17	49	20.20	58.78	41.22
40%	6	2955.2	13:43-15:10	87	37.75	56.61	43.39
30%	1	3806	10:32-11:48	76	12.57	83.46	16.54
30%	2	2804	10:15-11:23	68	21.27	68.73	31.27
30%	3	1008	13:48-15:14	86	69.20	19.53	80.47
30%	4	1136	10:20-11:20	60	41.07	31.56	68.44
30%	5	1541	13:36-15:04	88	62.32	29.19	70.81
30%	6	1784	10:22-11:11	71	41.27	41.88	58.12
25%	1	3843	13:36-14:54	78	13.95	82.12	17.88
25%	2	885	11:16-12:37	81	66.25	18.21	81.79
25%	3	1323	14:56-16:18	82	59.95	26.89	73.11
25%	4	2416	10:41-11:44	63	22.73	63.92	36.08
25%	5	390	14:00-15:40	100	93.50	6.50	93.50
25%	6	1924	10:48-11:56	68	35.93	47.16	52.84
20%	1	1397	14:11-15:19	68	44.72	34.24	65.76
20%	2	1019	10:31-11:27	56	39.02	30.33	69.67
20%	3	1020	13:42-14:37	55	38.00	30.91	69.09
20%	4	1421	10:11-11:19	68	44.32	34.83	65.17
20%	5	832	13:36-14:31	55	41.13	25.21	74.79
20%	6	1268	16:55-17:47	52	30.87	40.64	59.36

15%	1	1627	10:20-11:18	58	30.88	46.75	53.25
15%	2	1512	14:02-14:53	51	25.80	49.41	50.59
15%	3	1710	10:19-10:57	38	9.50	75.00	25.00
15%	4	2483	13:30-14:20	50	8.62	82.77	17.23
15%	5	2270	15:22-16:28	66	28.17	57.32	42.68
15%	6	1101	10:16-11:12	56	37.65	32.77	67.23
10%	1	1670	13:37-14:32	55	27.17	50.61	49.39
10%	2	1584	16:50-17:23	33	6.60	80.00	20.00
10%	3	1807	12:47-13:21	34	3.88	88.58	11.42
10%	4	2189	15:49-16:33	44	7.52	82.92	17.08
10%	5	1131	10:17-10:43	26	7.15	72.50	27.50
10%	6	783	13:05-13:40	35	21.95	37.29	62.71

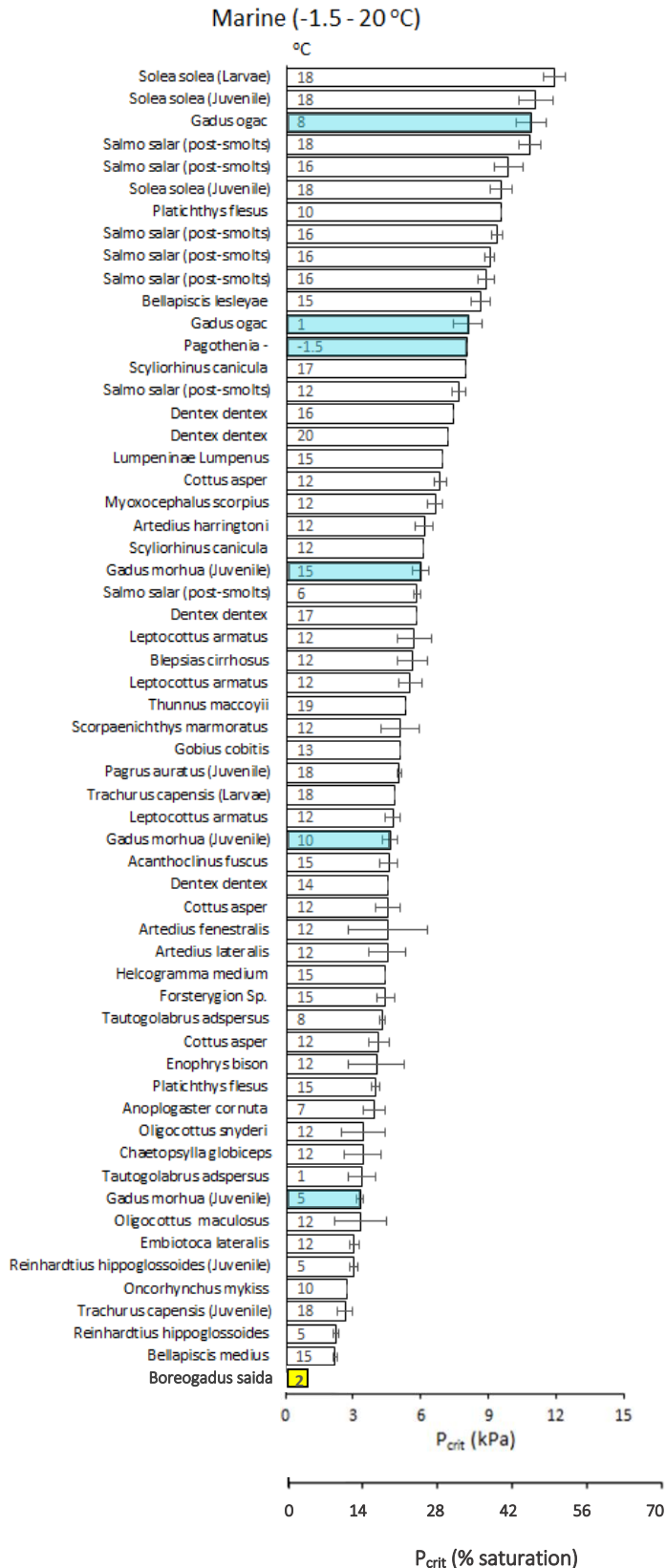


Figure 20 P_{crit} of marine species grouped by temperature range -1.5 to 20°C. Values represent the respective mean P_{crit} (± SE). Numbers contained within each bar indicate the temperature (°C) at which P_{crit} was determined. Blue shaded bars mark data of Polar- or Gadidae species, relevant for this study. Yellow bar: P_{crit} of *B. saida* determined in this study and included in this database (modified after Rogers et al. 2016).

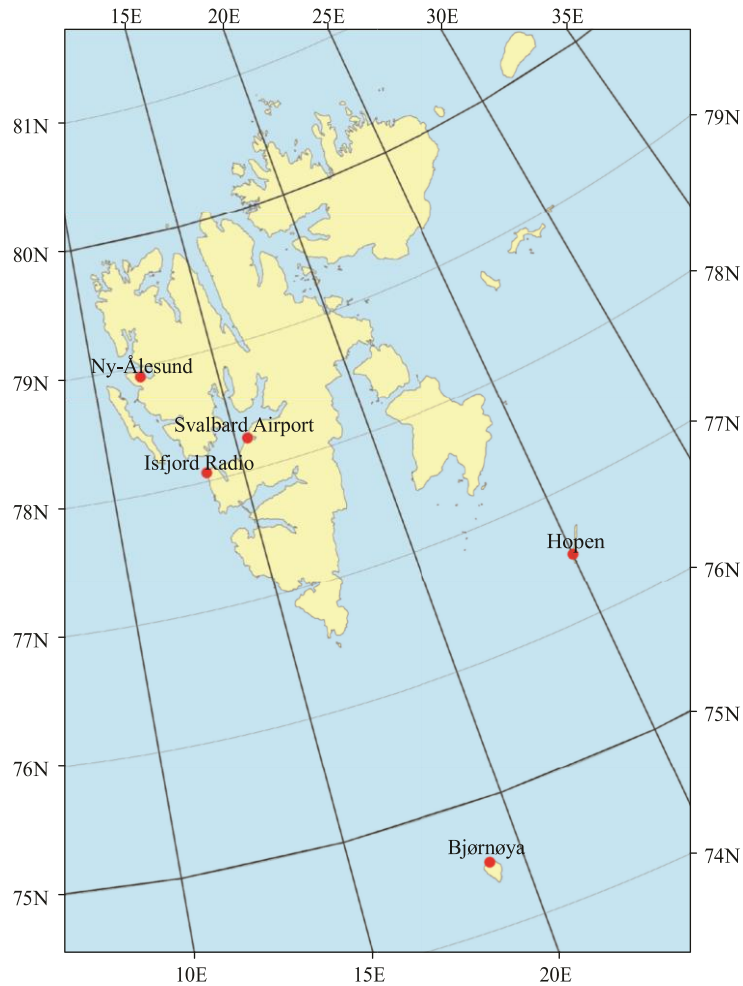


Figure 21 Map of the Svalbard region including weather stations used in the analysis (Førland, Benestad et al. 2011).

Table 11 Average annual and seasonal temperatures (°C) during 1961–90 and 1981–2010 (Førland, Benestad et al. 2011).

Station	1961–1990					1981–2010				
	Annual	Winter	Spring	Summer	Autumn	Annual	Winter	Spring	Summer	Autumn
Ny-Ålesund	-6.3	-13.8	-9.8	3.4	-5.3	-5.2	-12	-8.5	3.8	-4.4
Svalbard Airport	-6.7	-15.1	-10.8	4.2	-5.2	-4.6	-11.7	-8.3	5.2	-3.5
Hopen	-6.4	-13.4	-9.9	1.3	-3.8	-4.3	-9.9	-7.6	2.3	-1.9
Bjørnøya	-2.4	-7.6	-4.8	3.5	-0.5	-0.9	-5.1	-3.4	4.4	0.6

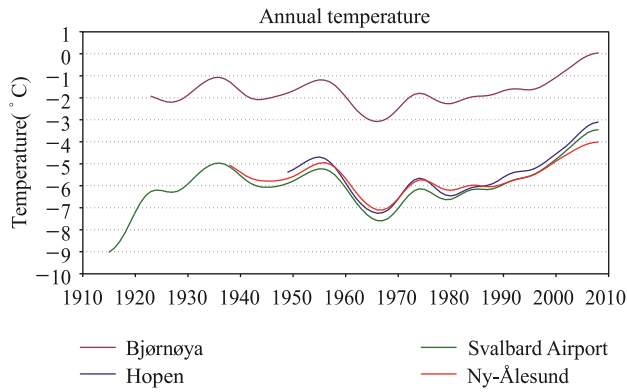


Figure 22 Annual temperature development at weather stations in the Svalbard region. The lowpass filtered series are smoothed by Gaussian weighting coefficients and show variability on a decadal time scale. The curves are cut three years from start and end (Førland, Benestad et al. 2011).

Table 12 RCM simulations for the Svalbard region. The simulations were performed by the regional climate model HIRHAM2/NorACIA (Førland, Flatøy et al. 2009, Førland, Benestad et al. 2011).

Global model	Emission scenario [35]	Control		Scenario	
		Period	Acronym	Period	Acronym
Max-Planck Inst.	IS92a	1981–2010	MPI92a	2021–2050	MPI92b
ECHAM4	SRES B2	1961–1990	MPICN	2071–2100	MPIB2
Hadley Centre	SRES A2	1961–1990	HADCN	2071–2100	HADA2
HadAM3H	SRES B2	1961–1990	HADCN	2071–2100	HADB2
Hadley Centre	SRES A1 B	1961–1990	HADA1	2021–2050	HADA1b
HadCM3	SRES A1B	1961–1990	HADA1	2071–2099	HADA1c

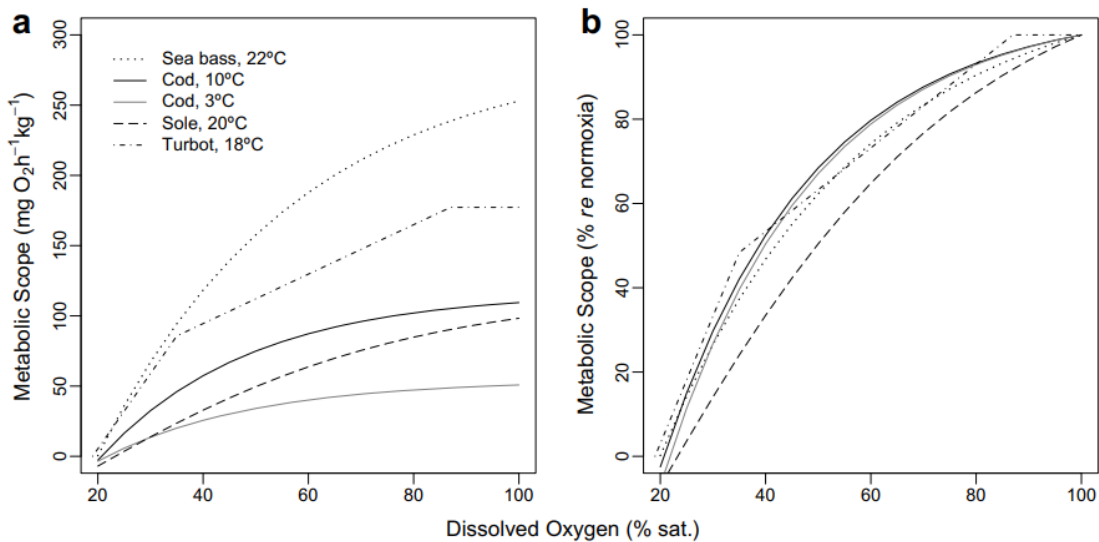


Figure 23 Collection of metabolic scopes of European sea bass (*Dicentrarchus labrax*), Atlantic cod (*Gadus morhua*), common sole (*Solea solea*) and turbot (*Psetta maxima*) as a function of ambient dissolved oxygen. MS is shown on absolute scale (a) and relative to normoxia (b) (Chabot and Claireaux 2008).

Acknowledgements – Danksagung

Im Verlauf dieser Masterarbeit bin ich vielen Menschen begegnet, denen ich auf unterschiedlichste Art und Weise dankbar bin:

Zunächst möchte ich mich gerne bei **Prof. Dr. Hans-Otto Pörtner** dafür bedanken, dass ich meine Masterarbeit in seiner Sektion durchführen durfte.

Dr. Andreas Kunzmann danke ich für die Zustimmung zur Erstellung eines Gutachtens dieser Arbeit.

Wieder einmal geht mein vielleicht größter Dank an **Dr. Felix Christopher Mark**. Danke Felix, dass Du nach mittlerweile drei Jahren immer noch mit mir zusammenarbeiten möchtest und mich im Oktober 2018 nach Spitzbergen bugsiert hast! Ohne diese Ausfahrt hätte ich nie so einen großen Gefallen an den kleinen Viechern gefunden und diese Arbeit wäre vielleicht nicht zustande gekommen. Außerdem ein riesiges, mit Sonnenstempeln versehenes Dankeschön 🌻🌻🌻🌻 für deine tolle Betreuung und Beratung, dein immer offenes Ohr und deinen kühlen Kopf, wenn uns die Technik mal wieder einen Strich durch die Rechnung machen wollte.

Darüber hinaus möchte ich mich gerne bei der gesamten **Sektion Integrative Ökophysiologie** für all die Unterstützung während meiner Versuche und bedanken. Mein besonderer Dank richtet sich hier an **Fredy Veliz Moraleda** und **Amirhossein Karamyar**, ich danke euch zu tiefst für euren Einsatz wenn es mal an der Zeit war meine Fische vor tropischen Temperaturen im Kühlraum zu retten, für eure Bastelkünste ohne die der Schwimmtunnel-Versuch nicht so leicht von der Hand gegangen wäre und nicht zuletzt für eure positive Einstellung und gute Laune wenn mal wieder Steine aus dem Weg zu räumen waren!

Ein großes Dankeschön richtet sich auch an **Corina Peter**, **Franziska Pausch**, **Kiara Franke** und **Thorsten Geller** ❤️, die mich alle auf unterschiedlichsten Weisen auf meinem Weg zur Beendigung meiner Masterarbeit unterstützt haben. Ihr habt mich in diesem Jahr sehr aufgebaut und ich bin sehr froh euch zu haben!

Sarah Kempf
Graudenzer Str. 30-34
28201 Bremen

Sarah Kempf

Name:

4194749

Enrolment number:

Declaration of copyright

Hereby I, Sarah Kempf, declare that my Master's Thesis was written without external support and that I did not use any other sources and auxiliary means than those quoted. All statements which are literally or analogously taken from other publications have been identified as quotations.

Bremen, 05.01.2020

Date:

Signature:

Declaration with regard to publishing theses

Two years after the final degree, the thesis will be submitted to the University of Bremen archive and stored there permanently.

Storage includes:

- 1) Master's Theses with a local or regional reference, as well as 10 % of all theses from every subject and year
- 2) Bachelor's Theses: The first and last Bachelor degrees from every subject and year

I agree that for research purposes third parties can look into my thesis stored in the University archive.

I agree that for research purposes third parties can look into my thesis stored in the University archive after a period of 30 years (in line with §7 para. 2 BremArchivG).

I do not agree that for research purposes third parties can look into my thesis stored in the University archive.

Bremen, 05.01.2020

Date:

Signature: